Contents list available at CBIORE journal website

International Journal of Renewable Energy Development

Journal homepage: https://ijred.cbiore.id

Research Article

Design and optimization of an energy storage system for off-grid rural communities

Zain Ul Abddin Soomro[a], Shoaib Ahmed Khatri[a*], Nayyar Hussain Mirjat[a], Abdul Hannan Memon[a], Muhammad Aslam Uqaili[a], Laveet Kumar[b]

[a]*Department of Electrical Engineering, Mehran University of Engineering and Technology, Jamshoro, 76062, Pakistan.*

[b]*Department of Mechanical and Industrial Engineering, College of Engineering, Qatar University, Doha, Qatar.*

Abstract. Access to reliable electricity remains a significant challenge in various developing countries, specifically in Pakistan, where traditional grid expansion is often economically unfeasible, especially in remote and rural areas, which results in frequent outages and limited access to modern energy services. To address this issue, this research aims to design and optimize an off-grid microgrid system powered by Renewable Energy (RE) sources, specifically solar energy, integrated with an efficient Energy Storage System (ESS) to ensure a continuous supply during low Solar Irradiance (I_h), adverse weather conditions, and at night. The proposed off-grid system includes three types of storage technologies: Lithium-Ion Battery (LIB), Sodium-Ion Battery (NIB), and Hydrogen Storage System (HSS). The study employs HOMER Pro to simulate and optimize the system sized as 150 kW. The comprehensive techno-economic analysis is undertaken, and offers two key perspectives, i) System #2 exhibits better technical performance, offering a higher RE fraction and capacity utilization, and ii) System #1 has better economic performance by providing lower Net Present Cost (NPC) and Levelized Cost of Energy (LCOE), Specifically, with the integration of NIBs. These results reveal that the 1.53 $M of NPC, 0.0649 $/kWh of LCOE are the lowest, at RE fraction of 100%, and 0.0977% capacity shortage with 0.0494% of unmet load respectively. A sensitivity analysis is also undertaken to establish the robustness of the proposed off-grid system and the impact of uncertain techno-economic parameters on NPC and LCOE with a variation of ±2%, which enhances the reliability in meeting energy demands. The primary objective of this research is to investigate the potential of NIBs as a future-forward energy storage option, being cost-effective, and derived from abundant, low-cost materials, i.e., Sodium (Na).

Keywords: Rural Community, Solar Photovoltaic, Energy Storage System, Optimization, Net Present Cost, Levelized Cost of Energy

Received: 10th March 2025; Revised: 26th Oct 2025; Accepted: 9st January 2026; Available online: 11th Feb 2026

1. Introduction

In today's era, humans cannot think of living without electricity. Due to population growth and rapid climate change, the world suffers greatly from the current and future energy demands (Khatri *et al.,* 2022). The global energy landscape is undergoing a significant transformation, driven by the urgent need for sustainable and reliable energy solutions (Mirjat *et al.,* 2018). In various developing countries, specifically in remote and rural areas, where access to electricity remains a significant challenge. According to the International Energy Agency (IEA) report, approximately 760 million people worldwide still lack access to electricity, with a significant proportion residing in rural communities (IEA, 2024). Among these regions, Pakistan stands out as one of the countries grappling with energy access challenges (Hussain Mirjat *et al.,* 2018). Approximately 17.5% of its population lacks access to electricity. This lack of access not only hampers socioeconomic development but also limits opportunities for education, healthcare, and overall quality of life (Alam *et al.,* 2021).

Traditional grid extension methods are often economically unfeasible in these regions due to high infrastructure costs and low population density. The off-grid solutions, particularly those based on RE sources, are viable alternatives for rural electrification (Justo *et al.* 2013; Sen and Bhattacharyya 2014). Solar energy is abundant and decreasing costs make it feasible for off-grid microgrid systems, making it an attractive option for rural communities (Patel & Singal, 2019). Solar energy systems can be deployed at various scales, from small households to larger community-based installations, providing flexibility to local energy needs (El Fathi & Outzourhit, 2018). Hybrid systems that combine solar and wind energy with ESS can further enhance the reliability and resilience of off-grid power supply (Kitson *et al.,* 2018). By leveraging local RE resources, rural communities can achieve energy self-sufficiency, reduce dependence on fossil fuels, and improve their overall quality of life (Nadaleti *et al.,* 2020).

ESS plays a crucial role in enhancing the reliability and efficiency of RE sources, specifically in off-grid microgrid applications, such as solar PV, which are inherently intermittent, leading to fluctuations in energy generation that can complicate their integration into the energy supply chain (Kumar *et al.,* 2019). ESS ensure a viable solution for energy independence, by harnessing local RE resources and storing energy that can be used during rough weather conditions. As a result, not only rural communities can reduce their reliance on fossil fuels but can enhance their energy security (Khan *et al.,* 2019). Deployment of ESS facilitates the diverse energy sources, enabling a more

* Corresponding author
Email: shoaib.ahmed@faculty.muet.edu.pk (S.A.Khatri)

https://doi.org/10.61435/ijred.2026.61191
ISSN: 2252-4940/© 2026.The Author(s). Published by CBIORE

resilient and flexible energy system (Nikolaidis & Poullikkas, 2017).

Challenges still abound in the optimization of ESS for off-grid rural communities. Where high capital costs for Battery Energy Storage (BES) technologies, especially LIB, result in financial obstacles for rural communities (Fodhil *et al.,* 2019). Moreover, there is a need to consider affordable alternatives for their energy supply without burdening the wallet. The most suitable BES technologies, such as Lead-Acid (LA), lithium-ion, flow batteries, or thermal systems, should be chosen based on cost, efficiency, durability, and environmental factors (Shaikh *et al.* (2025); Zakeri and Syri (2015)). The integration of ESS with RE sources requires careful planning, including optimization of energy generation and storage sizing (Gebrehiwot *et al.,* 2019). Simulation tools and optimization algorithms are used to find optimal configurations, and advanced control systems enhance the performance of ESS, extend its lifespan, and improve reliability (Luthander *et al.,* 2015). Ensuring socioeconomic benefits by improving access to ESS in off-grid areas, such as better education, economic development, and reduced reliance on Diesel Generators (DGs) (Ayodele *et al.,* 2014). The review from an environmental perspective is the ESS have potential to achieve the goals, by integrating with RE sources, reducing Greenhouse Gas (GHG) emissions, and promoting sustainable development (Seedahmed *et al.* (2022); Singh *et al.* (2022)).

The contemporary body of research has been dedicated to the design, optimization, and economic feasibility of microgrid and ESS, as shown in Table 1. Luta and Raji (2018) conducted a study in Napier, South Africa, based on the viability of grid extension versus development of an off-grid hybrid RE system by using HOMER Pro software. The study establishes a feasible microgrid system for electric supply to the area, and their findings revealed that under the current grid extension scheme, it wouldn't be an economical proposition for the targeted region to have a RE system versus grid extension. Kim and Jung (2018) analysed the most economical electrification methodology for an off-grid rural area in Myanmar using PV, DG, and BES configurations with both LA and LIB technologies, to determine the most economical solution, by using the HOMER Pro software tool to minimize the NPC of the system with best results for LA battery technology. Ayeng'o et al. (2018) analyses the PV, WT, DG, and BAT systems for Dodoma, Tanzania using both LA and LIB technologies to identify the most cost-efficient configuration and concluded with the LCOE for the LIB setup with the genetic algorithm is the lowest of all configurations.

Kaabeche and Bakelli (2019) compared the PV, WT, and BES systems using LA, LIB, and nickel-cadmium battery technologies in the Adrar province of Algeria, and performed optimization algorithms like GWO, ALO, Krill Herd, and JAYA on the system to reduce its electricity cost, and concluded that the LA battery-based design with the JAYA algorithm is the suitable solution as compared to LIB and Ni-Cd battery. Zia *et al.* (2019) presented the use of microgrids for rural area applications, focusing on oceanic islands like Ouessant Island of the coast of Brittany, France. The economic operation of a microgrid was obtained by combining the PV system, tidal turbine, DG, and LIB, accounting for the cost of degradation of the battery, LCOE, operating/emission costs of the DG, and network constraints. Li *et al.* (2020) conducted research on the WT, DG, and BESSs for 280 off-grid households in Gansu province, China, using LA, LIB, and Zinc–Bromine (ZB) battery technologies, by using the HOMER Pro software tool, and concluded that ZB battery technology offers the best option for the investigated system. Farinis and Kanellos (2021) proposed an Energy Management System (EMS) for microgrids and building prosumers using a multi-agent system, Particle Swarm Optimization (PSO), and thermal and electrical models. Zarate-Perez *et al.* (2022) used a systematic and bibliometric approach to evaluate the performance and challenges of integrating BESSs into microgrids, however, the optimization methods and cost-benefit analysis are key elements for developing an optimal BESS. The study also takes other considerations including reliability, BES technologies, power quality, frequency variations, and environmental conditions, where economic factors are the biggest challenges for battery ESSs.

Several authors have conducted techno-economic analyses of microgrid systems with various power providers and storage methods: Shahzad *et al.* (2017) presented a techno-economic study on hybridization of PV and biomass technologies to provide electricity for residential and farm loads in a small village in Punjab province, Pakistan. Kumar et al. (2017) discussed the exothermic and endothermic processes during absorption and adsorption in the HSS, which requires cooling and heating systems. Belkhiria *et al.* (2017) and Kumar et al. (2020) suggested various methods for increasing the efficiency of hydrogen discharge during FC operation that involve water heating and induction heating systems used for the preheating of the HSS in the process. Phurailatpam *et al.* (2018) used HOMER to evaluate the performance of a DC microgrid powered by solar, wind, and DGs for rural and urban loads in India. Mariama *et al.* (2018) proposed a microgrid system with RE sources and HSS to eliminate the problem of load shedding in Comoros, also developed and examined through HOMER. Von Colbe *et al.* (2019) identified in their study the effective means of storage for hydrogen PV-generated, including HSS and high-pressure cylinders. This development holds immense potential for various in overcoming energy access challenges in rural Pakistan, where 17.5% of the population remains without electricity.

Thus, the body of literature review shows that previous studies have focused on LA and LIBs for HRESs. However, these technologies face challenges in terms of cost, environmental impact, and availability of raw materials. Despite the recent developments in BES, there remains a lack of research done on NIBs to be adopted for off-grid rural electrification, meaning the benefit of NIBs in rural electrification has not been well exploited. This gap is substantial as NIBs are gaining global attention due to their cost-effectiveness, abundant raw materials (such as Na), and promising performance for RE storage.

It is, therefore, this study is designed to promote the achievement of sustainable off-grid energy solutions that can benefit the socioeconomic environment, ensure access to education, and support local economic activities worldwide. The main contributions of the proposed design assessment are as follows:

- Optimal design of RE system with ESS based off-grid microgrids, including PV, BES, FC, Electrolyzer (EL), HSS, and converter to minimize the NPC and COE by reducing unmet load, capacity shortage, and excess energy generation.
- Analyse the impact of the ESS, especially in terms of NIB, by minimizing the NPC and COE, while maintaining high reliability.

Based on the results, the most reliable, efficient, and economically viable method for rural electrification is to integrate RE systems with ESS in an off-grid microgrid.

This study presents a novel approach to introduce NIB technology into the techno-economic analysis of microgrids for rural electrification. It is a subject that has been largely overlooked in literature. By integrating NIBs into the modelling

Table 1
Summary of similar previous studies of HRES based on off-grid microgrid.

Author and Year	System Architecture	Grid Type	Location	Simulation Tool	Method	Objective	Performance Parameter
Dash *et al.* (2023)	WT/BG/Tidal/LIB	Off-grid	Andaman, Nicobar Islands, India	HOMER	Optimization	Minimize NPC, IC, emissions	Effective in emissions reduction
(Mulenga *et al.*, 2023)	PV-diesel	Off-grid	Zambia	HOMER	Optimization	Minimize LCOE, emissions	Cost-effective but diesel reliance
Hasan *et al.* (2023)	Wind-solar hybrid	Off-grid	Northeast Australia	HOMER	Optimization	Reduces emissions, affected by seasonal fluctuations	Reduces emissions, affected by seasonal fluctuations
Mulumba and Farzaneh (2023)	PV, WT, Flywheel, BES	Off-grid	-	MATLAB	Multi-objective optimization	Minimize LCOE, enhance reliability	High reliability under climatic situations
Wang and Grimmelt (2023)	Hydrogen-battery hybrid	Off-grid	-	HOMER	Simulation	Evaluate economic feasibility	Economical but diesel dependence
Moran *et al.* (2023)	Wind-solar, Grid-connected	Grid-connected	Ireland	TEA	Techno-economic analysis	Minimize LCOE, emissions	Cost-effective for grid use
Abd El-Sattar *et al.* (2022)	PV/WT/Biogas/FC	Off-grid	Egypt	PSO-GWO	PSO-GWO Hybrid Algorithm	Minimize NPC, maximize reliability	Improved load management
Shaikh *et al.* (2022)	WT/FC	Grid-connected	Urban China	HOMER	Optimization	Grid stability, minimize emissions	Enhanced grid stability
Jiang *et al.* (2022)	Solar-Geothermal-Battery	Hybrid-grid	Indonesia	MATLAB/Simulink	Optimization	Minimize LCOE, enhance reliability	High integration efficiency
Kapen *et al.* (2022)	WT/PV/BES/FC/Biodiesel	Off-grid	Malaysia	HOMER	Simulation	Minimize diesel usage, optimize renewables	Balanced and efficient energy use
Babatunde et al. (2022)	PV/DG/BES	Off-grid	Remote regions	HOMER	Optimization	Minimize COE, maximize reliability	Optimized sizing
Zarate-Perez *et al.* (2022)	PV/WT/BES/FC	Off-grid	Bangladesh	MATLAB/Simulink	Artificial Neural Networks	Maximize reliability, minimize cost	High reliability, lower NPC
Boglou *et al.* (2022)	PV/BES/Diesel Generator	Off-grid	Remote villages in Pakistan	HOMER	HOMER	Minimize COE, optimize energy dispatch	Balanced energy supply
Yang e*t al.* (2008)	WT/Biomass/FC	Off-grid	Iran	PSO	PSO	Minimizing total system cost, optimal sizing	Moderate stability
Ma *et al.* (2023)	PV/WT/FC	Stand-alone	China	Modified NSGA-II	Modified NSGA-II	Minimizing COE, LOPSP, and PAR	Improved reliability
Sultan *et al.* (2021)	PV/ WT/FC/BES	Off-grid	Iran	HOMER	HOMER, Complex proportional assessment	Minimizing NPC	Moderate reliability
El-Sattar *et al.* (2022)	PV/Biomass/FC	Off-grid	Egypt	Mayfly Optimization Algorithm	Mayfly Optimization Algorithm	Minimize COE, Maximize reliability	High reliability
Samy *et al.* (2020)	WT/PV/FC	Isolated	Egypt	Firefly Algorithm	Firefly Algorithm	Minimizing NPC	Resilient, low cost
Ishraque *et al.* (2021)	WT/BES/DG	Stand-alone	Australia	HOMER	Simulation	Maximize system resilience, minimize emissions	Reliable, environmentally friendly
Ahmed and Karthikeyan (2018)	WT/PV/BES/FC	Isolated	Rural Nepal	HOMER	Simulation	Minimize COE, ensure energy reliability	Balanced energy supply
Zhang *et al.* (2019)	PV/WT/FC	Off-grid	Iran	Custom ANN	CS-HS-SA-ANN	Techno-economic and sizing	Moderate reliability
N'guessan *et al.* (2020)	WT/FC/BES/SC	Isolated	China	NSGA-II	NSGA-II	Minimizing TAC and LOPSP	High resilience
Jahannoosh *et al.* (2021)	WT/PV/FC	Isolated	Iran	HGWOSCA	HGWOSCA	Minimizing lifecycle cost, maximizing reliability	Extended lifecycle
Sultan *et al.* (2021)	WT/PV/FC	Off-grid	Egypt	IAEOA	IAEOA	Minimizing COE	Cost-effective
Masrur *et al.* (2020)	WT/PV/DG/BES	Stand-alone	Bangladesh	HOMER	HOMER	Techno-economic feasibility	High techno-economic balance
Kamran *et al.* (2018)	PV/WT/BES/FC	Off-grid	Pakistan	Fuzzy logic control	Fuzzy logic	Minimize energy storage degradation	High flexibility
Ma *et al.* (2023)	PV/BES	Islanded	Remote islands	Modified NSGA-II	Multi-objective optimization	Minimize COE, emissions	Eco-friendly and reliable

Table 2 (Cont'd)
Summary of similar previous studies of HRES based on off-grid microgrid.

Memon and Patel (2021)	Solar-thermal/Wind-turbine	Hybrid	Australia	TRNSYS	Energy analysis	Maximize efficiency, minimize waste heat	High thermal efficiency
Zhang *et al.* (2018)	PV/WT/BES/FC	Isolated	Iran	SCHSA	SCHSA	Optimal sizing	High-cost efficiency
Das *et al.* (2019)	PV/BG/PHS/BES	Off-grid	India	Water Cycle Algorithm	Water cycle algorithm	Minimizing NPC, Optimal sizing	High reliability
Sanajaoba (2019)	WT/PV/BES	Stand-alone	India	Firefly Algorithm	Firefly algorithm	Minimized COE	High economic efficiency
Jahannoush and Nowdeh (2020)	WT/PV/FC	Off-grid	Iran	Sine-cosine Algorithm	Improved sine-cosine algorithm	Minimized lifecycle cost of hybrid system	High stability
Moghaddam *et al.* (2019)	WT/PV/FC	Off-grid	Iran	Flower Pollination Algorithm	Intelligent flower pollination algorithm	Minimize NPC, optimal sizing	Reliable cost reduction
Babatunde *et al.* (2022)	PV/WT/BES/FC	Off-grid	Africa	HOMER	HOMER	Minimizing NPC and COE	High reliability, low COE
Kapen *et al.* (2022)	PV/Biogas/BES/FC	Off-grid	Cameroon	HOMER	HOMER	Minimizing NPC and COE	High system efficiency
Ghorbani *et al.* (2018)	WT/PV/BES	Off-grid	Iran	GA-PSO	GA-PSO	Minimized NPC	High economic efficiency
Abdin and Mérida (2019)	WT/PV/BES/FC	Off-grid	Canada, USA, Australia	HOMER	HOMER	Sizing and techno-economic analysis	Broad application
Jiang *et al.* (2022)	WT/PV/FC/BES	Off-grid	China	Improved GA-PSO	Improved GA-PSO	Optimal sizing	High design efficiency
Ngila and Farzaneh (2023)	PV/WT/Flywheel/BES	Stand-alone	Kenya	MATLAB Simulink	MATLAB Simulink	Optimal sizing	Stable, high reliability
Bakhtiari and Naghizadeh (2018)	PV/WT/BES/FC	Stand-alone	-	Shuffled Frog Algorithm	Shuffled frog leaping algorithm	Optimal design	High system performance

and optimization framework, this research not only addresses the financial and environmental limitations of traditional batteries but also paves the path towards future adoption of NIBs in developing countries. This is one of the first studies to assess the potential of NIBs as a cost-effective, scalable, and sustainable energy storage solution for off-grid rural electrification systems.

The rest of the paper is organized as follows: Section 2 discusses the materials and methodology. The mathematical modelling of the microgrid system is presented in Section 3. Section 4 presents the simulation and the objective function. Section 5 presents the results and analysis. Lastly, the conclusions are drawn in Section 5

2. Methods

The research methodology undertaken for this study, has the objective of minimizing the NPC and LCOE, as well as to analyse the potential of NIB for off-grid systems. To accomplish this, the study uses HOMER Pro tool for the design, simulation, and optimization of the system, with load demand and metrological data of the study site (village 'Ruk,' Shikarpur, Pakistan). The detailed description of the off-grid system, materials and methodology is provided in the following section.

2.1. Proposed research design

The proposed research design for this study is centred on enhancing the effectiveness of an optimized ESS, and customized to meet the specific requirements of rural off-grid communities. Fig 1, Shows the comprehensive methodological approach for modelling and analysing the off-grid RE system,

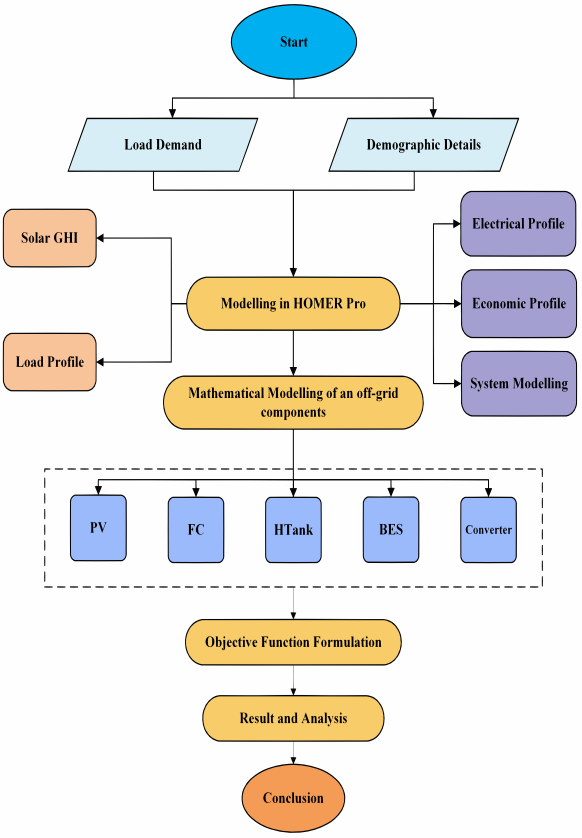

Fig 1. Framework for proposed research.

Fig 2. The location of the study area on the map.

integrating simulation and mathematical approach. The flow diagram starts with the data collection, including load demand and demographic details. Furthermore, HOMER Pro tool is used for modelling, which requires the solar Global Horizontal Irradiance (GHI) and load profile, along with the development of electrical, economic, and system profiles. The parameters will be used as input for system modelling and optimization. To establish the reliability and accuracy, the mathematical modelling is further employed to incorporate individual system components, such as solar PV, Fuel Cell (FC), Hydrogen Tank (HTank) storage, BESSs, and power converters. The subsequent objective function formulation enables optimization of system performance based on defined criteria. As such, the methodological approach concludes in a detailed result and analysis phase, leading to a convincing evaluation of the system's viability and effectiveness.

It is envisaged that the proposed research framework may bridge the gap that exists in the ESS for an off-grid microgrid system and provide a robust and systematic approach for the design, simulation, and optimization, as well as ensuring accurate performance assessment and informed decision-making for sustainable energy planning.

2.2. Demographics Details

Solar energy is available for the remote village 'Ruk,' Shikarpur, Pakistan, at 27.857522490694546 N latitude and 68.65054323173707 E longitude. A total of 860 people live in the study area, with an average of 5 people living in a household for 172 households. Fig 2, shows the geographic location of the study area on the map.

The remote area is facing electrification issues, because of financial instability, and cannot afford expensive electricity, as a result 50% of the population is living without electricity, people still live with lighting candles, and kerosene lanterns, and it has been observed that very few houses are using solar-PV panels lamps and fans.

2.3. Load Profile

The electrical load profile is a critical factor that needs to be considered while sizing and designing a distribution system. In this study, the load profiles of the study area (Rural community) have been achieved by physical survey, as illustrated in Table 2. The field survey was conducted to determine the various types of loads in the domestic, community, agricultural, and commercial sectors. The total load demand for rural communities is 14.610 kW when the 100% load is connected.

The aggregated load profile, consisting of domestic, commercial, community, and agricultural load demands, results in a total peak load of 145.61 kW, which necessitates a reliable energy system and ensures a continuous and balanced power supply across all sectors.

2.4. Modelling Using HOMER Pro Software

This section presents a comprehensive outline of all the necessary details for undertaking simulations using HOMER Pro the HOMER Pro simulation tool, initially created by the National Renewable Energy Laboratory (NREL) based in the United States, to conduct analysis and optimization. Key input parameters, comprising resource data, load data, area location, and project parameters, hold fundamental significance for the tool's seamless functioning. With this information, HOMER Pro systematically explores various system configurations and consciously selects the most suitable one by minimizing both

Table 3
Organization and classification of types of loads

Apparatus	Appliances	Ratings (W)	Connected Devices	Total (W)
Domestic Loads				
Household (172)	Lights	20	1550	31000
	Fans	60	516	30960
	Television	100	70	7000
	Air Conditioner	1200	28	33600
Total Domestic Load				**102560**
Commercial Loads				
shops (35)	Lights	20	70	1400
	Fans	60	50	3000
	Television	100	10	1000
	Refrigerator	150	25	3750
Flour Mill	-	2000	2	4000
Sawmills	-	3000	1	3000
Total Commercial Load				**16150**
Community Loads				
Hospitals	Lights	20	35	700
	Fans	60	15	900
	Refrigerator	150	2	300
	Cooler	250	1	250
School (4)	Lights	20	200	4000
	Fans	60	100	6000
	Computer	250	35	8750
Total Community Load				**20900**
Agriculture Load				
	Water Pump	1500	4	6000
Total Load				**145610**

the NPC and COE. Furthermore, this section delves into precise specifications for each component, facilitating a comprehensive understanding of the simulation process as shown in Fig 3. The flowchart presents the HOMER Pro modelling process used to design and optimize an off-grid Hybrid Renewable Energy System (HRES). This flowchart outlines the step-by-step approach taken to input, simulate, and analyse various RE configurations to meet the needs of rural, off-grid communities.

The process begins with the collection of essential inputs such as site-specific I_h, temperature data, and the estimated load demand. As a result, HOMER Pro runs simulations using this data to assess various configurations of energy sources, such as solar PV, batteries, and other components. Each configuration is evaluated based on metrics including NPC and LCOE, along with considerations for reliability and emissions. The flowchart then depicts how HOMER Pro ranks these configurations, selecting those that meet minimum NPC and LCOE requirements to provide an economically and technically viable energy solution.

The final step in the process involves the analysis and interpretation of results. HOMER Pro provides detailed outputs, including economic, technical, and environmental metrics for each configuration. These outputs help identify the optimal system design that balances cost-effectiveness, reliability, and sustainability. Insights from this analysis can also guide further refinement of the model, ensuring that the selected configuration is tailored to the specific energy needs and constraints of the rural community. By systematically following the flowchart, the study ensures a structured approach to designing efficient and practical off-grid energy systems.
It is anticipated that the process concludes with the ranking of feasible microgrid configurations based on minimum NPC and COE, as well as techno-economic and emission results.

2.5. HOMER Pro Software Inputs

The ambient temperature and solar irradiance data are obtained from NASA-SSE satellite datasets incorporated with the HOMER Pro database, for the selected geographical location. The averages of temperature, solar irradiation, and clearness index are depicted in Figure 4.

However, the average maximum temperature, recorded in 8 months (March, April, May, June, July, August, Sep, and Oct), ranges from 35-45 °C, and it seems that solar irradiance is also high in those 8 months, which range from 5.2-7.1 kWh/m^2/day, and relatively, the clearness index is at 0.63-0.7. Rest of the 4 months (Jan, Feb, Nov, and Dec), the minimum average temperature ranges from 15-30 °C, the solar irradiance ranges from 3.8-4.3 kWh/m^2/day, and the clearness index ranges from 0.59-0.62, as illustrated in Fig 4 (a) and (b). It is emphasized that the clearing index is the sum of the solar radiation on Earth's surface divided by the extra-terrestrial radiation at the top of the atmosphere.

The electrical P_{Load} is estimated hourly for a remotely located 'Ruk' village with 172 households. The four majors P_{Load}

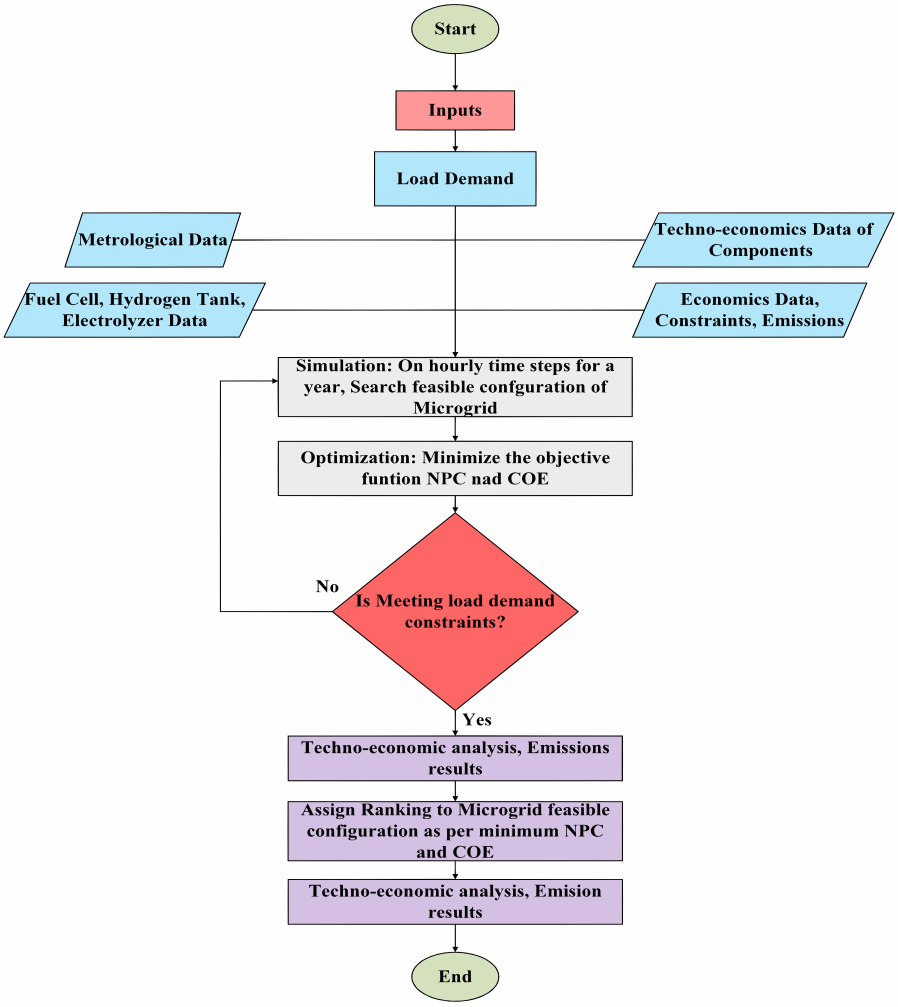

Fig 3. Flowchart of the HOMER Pro process

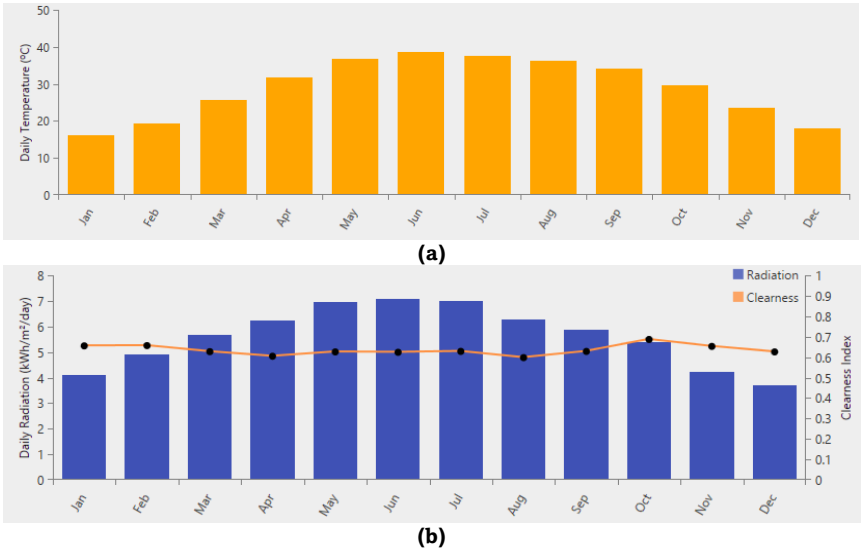

Fig 4. Metrological data, a) Ambient temperature, b) Solar irradiation and clearness index.

areas are domestic, commercial, community, and agricultural. The electrical equipment considered for load estimation and their ratings are presented in Table 2. Fig 5(a) represents the monthly average load profile, and Fig 5(b) depicts the hurly P_{Load}. The peak load is observed in August at 201.18 kW due to the summer season, and the lowest energy requirement is observed in January, February, and December due to the winter season when cooling loads are switched off. HOMER accumulates an array of 8760 hourly values of P_{Load} data from the specific daily profile of the study site, and afterward

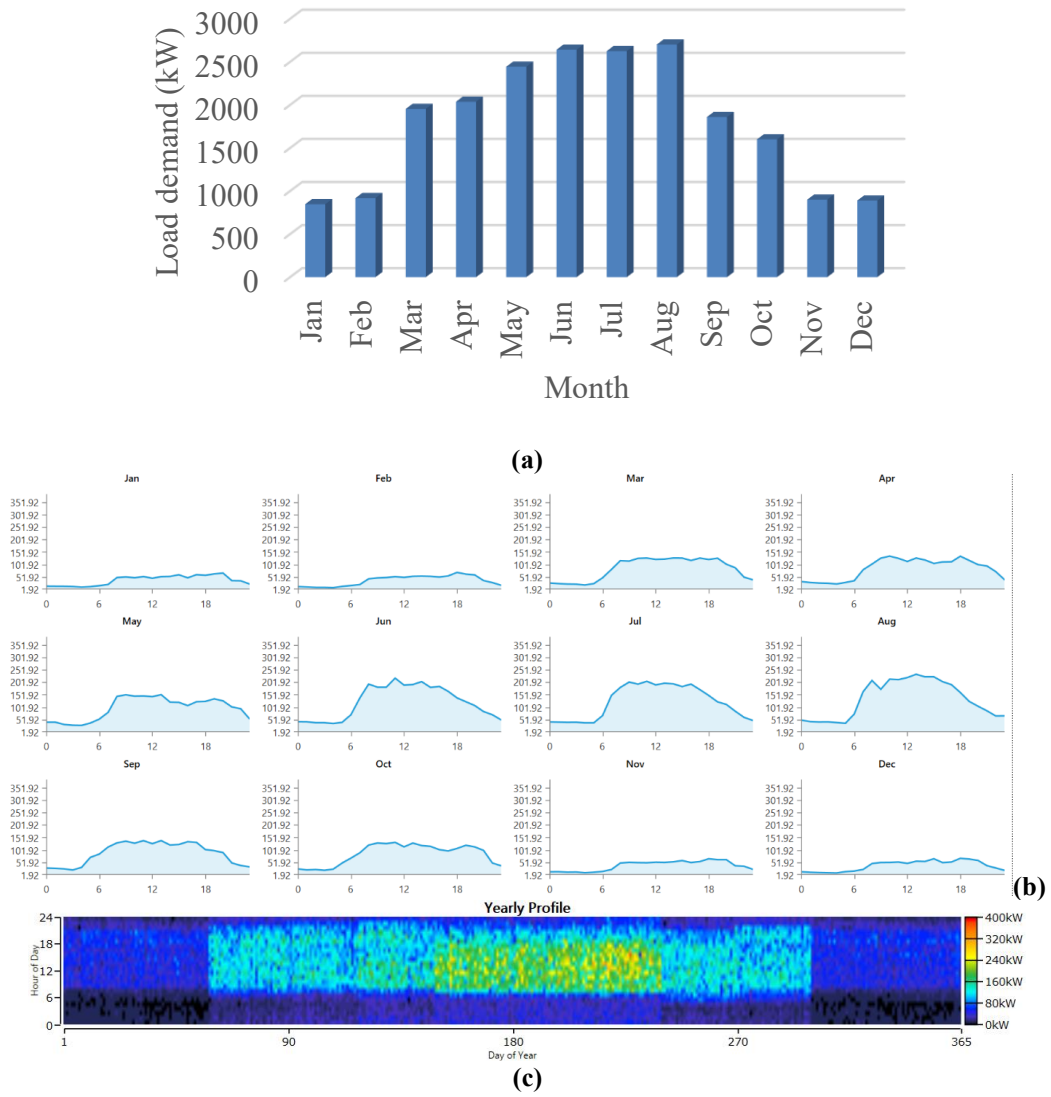

Fig 5. Load demand, a) monthly, b) daily, and c) yearly load profile with perturbation factors.

Table 4
Details of an off-grid system

Configuration	System #1		System #2	
	Case #1	Case #2	Case #3	Case #4
Off-Grid System	PV/NIB/EL/FC/HSS	PV/NIB	PV/LIB/EL/FC/HSS	PV/LIB

multiplies each hour's worth by a factor (α_{Ld}) to consider the load growth (Abdin and Mérida (2019); Al-Sharafi et al. (2017)):

$$\alpha_{Ld} = 1 + \delta_d + \delta_h \quad (1)$$

where, $\delta_h = 10\,\%$ and $\delta_d = 20\,\%$ are perturbation factors hourly and daily, respectively.

The yearly load profile variation with consideration of perturbation factors is shown in Fig 5(c). With perturbation factors, the peak load rises to 400 kW. Therefore, the HOMER Pro input dataset for the remote area simulation is undertaken with thorough attention to climatic and demand-side parameters. The favorable solar irradiance throughout the year, as well as detailed and survey-based load estimation incorporating future growth factors, ensures a comprehensive foundation for HRES design. Therefore, these inputs will directly influence techno-economic optimization and sustainability outcomes.

2.6. System configuration

The system configuration involves Solar PV, EL, FC, HTank, and batteries (NIB and LIB), as shown in Figure 6 (a), (b), (c), and (d), which presents the proposed off-grid microgrid layout at the site. It considers two system configurations with four cases. Also, see Table 3.

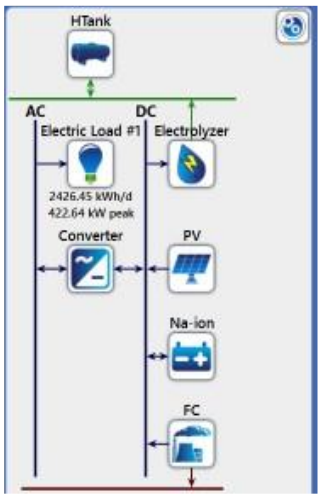

(a) Case #1: PV/NIB/EL/FC/HTank

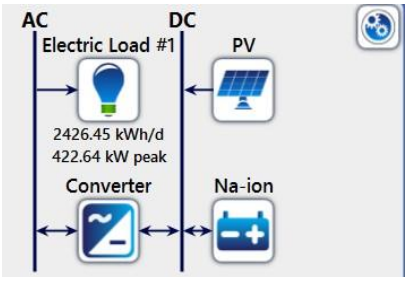

(b) Case #2: PV/NIB

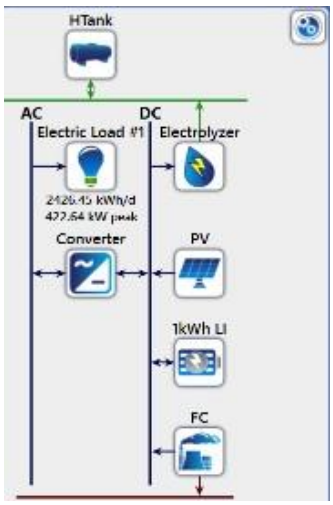

(c) Case #3: PV/LIB/EL/FC/HTank

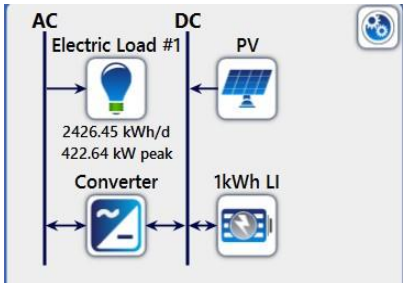

(d) Case #4: PV/LIB

Fig 6. Microgrid configuration (a) Case #1: PV/NIB/EL/FC/HTank, (b) Case #2: PV/NIB, (c) Case #3: PV/LIB/EL/FC/HTank, and (d) Case #4: PV/LIB.

Fig 6 (a) and (b) illustrate two cases of microgrid configurations for system #1. Case #1 incorporating Solar PV, a NIB, EL, FC, and HSS. This involves a multi-step process, starting with solar energy generation by PV panels, followed by excess energy storage in the LIB. Subsequently, the EL utilizes electricity to split water into hydrogen and oxygen, which is then stored in the HTank. The stored hydrogen powers the FC to generate electricity and supply it to the electric load. However, Case #2 represents a simplified configuration consisting solely of PV panels and a LIB. This system directly utilizes solar energy to power the electric load, with excess energy stored in the NIB for later use.

Fig 6(c) and (d) also presents the two cases of microgrid configurations for System #2. Case #3 incorporating PV, a LIB, EL, FC, and HSS. The process is the same as system #2, however, the only difference is BESS. As such, in this system, the LIB is used for storage in case #4. To evaluate the performance, feasibility, and efficiency of an off-grid microgrid system, comparative analysis has been undertaken for different BES technologies with HSS integration strategies.

2.7. Economics

The project lifetime (T_p) is taken 25 years, with the discount rate (D_r) of 8 % and an inflation rate (I_f) of 2 %, which is the present annual average I_f in Pakistan for the financial year 2023–24, i.e., October 2023 to September 2024 (Manoo *et al.,* 2024).

3. Mathematical modelling of off-grid microgrid components

The mathematical modelling and formulation of microgrid components are discussed below.

3.1. Solar PV

The electrical power produced from solar PV panels depends on the solar irradiance calculated by HOMER Pro. The power generated from solar PV ($P_{S,pv}$) is computed as (Aziz *et al.* (2019); Kumar *et al.* (2022); Singh et al. (2016)):

$$P_{S,pv}(t) = P_{RI,pv} \times d_{loss,pv} \times (I_h(t)/ I_{STC}) \times [1 + \alpha_{T,pv}(T_c - T_{STC})] \quad (2)$$

where, $d_{loss,pv}$ represents the derating factor for PV panels, I_h refers to solar irradiation on an hourly average, I_{STC} indicates the solar irradiation at STC, $\alpha_{T,pv}$ represents the temperature coefficient, T_c refers to the temperature of the PV cell, T_{STC}represents the temperature of the PV cell at STC and $P_{RI,pv}$ represents the rated power of a solar PV panel.

At night, $T_c = T_\alpha$ (ambient air temperature); however, in day hours, $T_c > T_\alpha$ by approximately 30 ℃ or more. The T_c is given as (Aziz et al. (2019); Kumar et al. (2022)):

$$T_c(t) = T_a(t) + T_{c,Noct} - T_{a,Noct} \times (I_h(t)/ I_{T,Noct}) \times \left(1 - {\mu_{mp}}/{\zeta_\varphi}\right) \quad (3)$$

where, $T_{a,Noct}$ represents the ambient temperature at the nominal operating cell temperature, $T_{c,Noct}$ is the nominal operating cell temperature, $I_{T,Noct}$ refers to solar irradiance at $T_{a,Noct}$, μ_{mp} denotes the solar PV system's efficiency at its maximum power point, ζ is solar transmittance, and φ represents the PV array's solar absorptance. The techno-economical parameters of the solar PV used in the study are shown in Table 4.

The techno-economic characteristics of the PV modules, serving as essential inputs for precisely modelling and evaluating the system's performance in the HOMER Pro environment.

3.2. Electrolyzer, HSS, and FC

The EL is responsible for producing hydrogen gas by consuming electrical energy. Mathematical, described as (Gharavi *et al.* (2015); Sultan *et al.* (2021)):

$$P_{Eler,Tank} = P_{Rer,Eler} \times \eta_{Eler} \quad (4)$$

where, $P_{Rer,Eler}$ represents renewable power supplied to the electrolyzer (kW), η_{Eler} refers to EL efficiency, and $P_{Eler,Tank}$ represents the power supply from the EL to the HSS.

The state of charge of an HSS ($SOC_{Tank}k$) is described as:

$$SOC_{Tank}(\boldsymbol{t}) = SOC_{Tank}(t-1) + (\boldsymbol{P}_{Eler,Tank}(t) - \frac{\boldsymbol{P}_{Tank,FC}(t)}{\eta_{Tank}}) \times \Delta t \quad (5)$$

where, $\boldsymbol{P}_{Tank,FC}$ represents power supplied from the HSS to the proton exchange membrane fuel cell (PEMFC), η_{Tank} represents the efficiency of HSS (~95 %), and Δt shows the time interval of 1 h.

The quantity of energy stored in the HSS is a function of the hydrogen mass (M_{Tank}), given as:

$$M_{Tank}(t) = \frac{SOC_{Tank}(t)}{HHV_H} \quad (6)$$

HHV_H refer to the higher heating value of hydrogen gas (=37.9 kWh/m^2).

During the operation, M_{Tank} should be kept within the minimum ($M_{Tank,Min}$) and maximum ($M_{Tank,Max}$) boundaries as:

$$M_{Tank,Min} \leq M_{Tank,k(t)} \leq M_{Tank,Max} \quad (7)$$

The power output of PEMFC is defined as [61]:

$$P_{FC} = P_{Tank,\boldsymbol{FC}} \times \eta_{FC} \quad (8)$$

where, η_{FC} represents the electrical efficiency of PEMFC. The techno-economic components of the EL, HSS, and FC are presented in Table 5 (Kapen *et al.* (2022); Sultan *et al.* (2021)).

The key techno-economic input parameters for modelling, such as EL, HTank, and FC, will ensure accurate simulation of the hydrogen-based energy storage and conversion systems in the proposed microgrid.

3.3. Battery Energy System (BES)

The idealized battery models are used in this study for energy storage. The charging of the battery is described in Eq. (10). Similarly, discharging the battery is described in Eq. (11) as (Askarzadeh and dos Santos Coelho (2015); Kapen et al. (2022)):

$$SOC_b(t) = SOC_b(t-1) \times (1-\tau)\ (P_{WT,G}(t) \times \eta_{con} + P_{S,pv}(t) - P_{Rer,Eler}(t) - \frac{P_{Load(t)}}{\eta_{con}}) \times \eta_{bch} \quad (9)$$

$$SOC_b(t) = SOC_b(t-1) \times (1-\tau) - (\frac{P_{Load(t)}}{\eta_{con}} - P_{FC}(t) - P_{S,pv}(t) - P_{WT,G}(t) \times \eta_{con})/\eta_{bdh} \quad (10)$$

Table 5
Cost and technical specification of PV

Parameters	Equation	Values	Units
Capital Cost	-	120	$/kW
Replacement Cost	-	115	$/kW
Operation & Maintenance Cost	-	4	$/year
De-rating factor	$d_{loss,pv}$	88	%
Lifetime	-	25	Years
Slop	--	26.04	Degree
Rated Power	$P_{RI,pv}$	0.325	kW
Open Circuit Voltage	Voc	45.82	V
Short Circuit Current	Isc	9.03	A
Maximum Power Voltage	Vpm	37.56	V
Maximum Power Current	Ipm	8.52	A
Efficiency	-	19.1	%
temperature of PV cell at STC	T_{STC}	25	℃
temperature coefficient	$\alpha_{T,pv}$	-0.39	%/℃
The ambient temperature at nominal operating cell temperature	$T_{a,Noct}$	20	℃
The nominal operating cell temperature	$T_{c,Noct}$	25	℃
Solar irradiation at STC	I_{STC}	1	kW/m^2
Solar irradiance at $T_{a,Noct}$	$I_{T,Noct}$	0.8	kW/m^2

Table 6
Cost and technical specification of EL and HTank

Components	Units	Electrolyzer	Hydrogen Tank	Fuel Cell
Capital Cost	$/kW	1100	1000	3000
Replacement Cost	$/kW	825	750	2700
O&M	$/kW-Year	16.5	N/A	100
Density	Kg/m^3			0.790
Fuel Price	$\$/m^3$			0.179
Carbon Content	%	N/A	N/A	63
Sulphur Content	%	N/A	N/A	0
Low Heating Value	MJ/kg	N/A	N/A	45
Capacity	kW	N/A	N/A	250
Density	Kg/m^3	N/A	N/A	0.790
Lifetime	Year or Hours	25	25	50,000
Efficiency	%	85	95	N/A

Table 7
Cost and technical specification of BES

Components	Units	Generic Lithium-Ion	Generic Sodium-Ion
Capital Cost	$	550	300
Replacement Cost	$	550	270
O&M	$/kW	0	0
Nominal Capacity	Ah	167	200
Voltage	V	12	12.4
Maximum Charge Current	A	167	200
Roundtrip Efficiency	%	95	97
Initial Hours (SOC_b)	%	100	100
Minimum Charge	%	20	20
DOD	%	90	95
Lifetime	years	25	25

where, τ indicates the self-discharge rate of a battery, η_{bch} refers to the charging efficiency of the battery, η_{bdh} represents battery discharging efficiency, and η_{con} is the converter's efficiency.

The battery can be discharged up to the minimum SOC_b level (SOC_b^{Min}), evaluated based on battery depth of discharge (DOD_b) as follows (Dargahi *et al.,* 2014):

$$SOC_b^{Min} = (1 - DOD_b) \times C_{bt} \quad (11)$$

where, C_{bt} represents the capacity of the battery.
The techno-economic components of BES are depicted in Table 6.

The detailed techno-economic characteristics of the two battery BES technologies, generic LIB and NIB provide a basis for comparative analysis in the context of performance, economics, and suitability for an off-grid microgrid integration.

3.4. Converter

The converter capacity should be designed to supply the peak load demand (P_{load}^{Max}) even with no power output on the AC bus. The converter capacity is determined as (Konneh *et al.* (2023); Singh *et al.* (2016)):

$$P_{con}(t) = \frac{P_{load}^{Max}(t)}{\eta_{con}} \quad (12)$$

where, η_{con} represents converter efficiency. The techno-economic components of the converter are depicted in Table 7. (Singh *et al.*, 2016).

However, the data highlights the cost and performance metrics of the power converter, with a lifecycle of 25 years and efficiency of 95%, which ensures the reliable and efficient operation of the microgrid system.

Table 8
Cost and technical specification of power converter

Parameters	Values	Units
Capital Cost	127	$/kW
Replacement Cost	114	$
Operation & Maintenance Cost	0	$/year
Lifetime	25	Years
Efficiency, η_{con}	95	%
Relative capacity	100	%

3.5. Objective function formulation

The simulation and optimization are performed on HOMER Pro to minimize the NPC and COE. To reduce the NPC, COE, and unmet load, HOMER Pro offers the best component sizing for the system (Abdin & Mérida, 2019). Techno-economic analysis simultaneously considers the rise in the cost of microgrid components. To evaluate the NPC, the annual I_f and nominal interest rate (In) are taken based on the on-site location. In HOMER, the NPC is assessed as:

$$NPC = \sum_{Tp=1}^{T_p=25} D_r(C_{cap} + C_{Rep} + C_{OM} - C_{Sv}) \quad (13)$$

where, $C_{cap}$is the capital cost, C_{Sv}, and C_{Rep} represent the microgrid components salvage value and replacement cost, respectively.

The discount rate (D_r) is evaluated as (15) (Abdin & Mérida, 2019), and the annual real interest rate (i_r) is evaluated based on the nominal i_r and I_f as follows (Al-Sharafi *et al.* (2017); Moghaddam *et al.* (2019)):

$$D_r = \frac{1}{(1+i_r)^{T_p}} \quad (14)$$

$$i_r = \frac{i_n - I_f}{1+I_f} \quad (15)$$

The annualized cost of microgrid components (C_{An_Tot}) is evaluated from NPC and using the Capital Recovery Factor (CRF) (Al-Sharafi *et al.* (2017); Yang *et al.* (2008)) as:

$$C_{An\_Tot} = CRF(i_r, T_p) \times NPC \quad (16)$$

$$CRF(i_r, T_p) = \frac{i_r(1+i_r)^{T_p}}{(1+i_r)^{T_p}-1} \quad (17)$$

The COE, expressed as the ratio of total annualized cost and total annual electrical energy (E_{Tot}) served to the load, is expressed as (19) (Chauhan & Saini, 2016). It displays the price per unit of useful energy generated by various generating units.

$$COE = \frac{C_{An\_Tot}}{E_{Tot}} \quad (18)$$

The Cost of Hydrogen (COH) is evaluated for an isolated system as follows:

$$COH = \frac{C_{An\_Tot} - V_{elec}(P_{Load}+P_{def})}{M_{H_2}} \quad (19)$$

where, V_{elec} represents the value of electricity, P_{def} shows the deferrable load, and M_{H_2} represents total hydrogen gas production.

4. Result and analysis

The proposed off-grid system for a remote village 'Ruk' in Sindh, Pakistan, includes PV, ESS (BES, EL, FC, and HSS) for backup power supply. The HOMER Pro obtains an optimal microgrid configuration, minimizing NPC and COE. The system's performance is evaluated at a maximum capacity shortage of 0 % with a cycle charging dispatch strategy.

4.1. Optimization results

The performance evaluation of the proposed off-grid microgrid is presents comparison of four configurations across two main system architectures. System #1 with hydrogen storage and system #2 without hydrogen. Where each system is evaluated with either NIB or LIB. However, as mentioned in Section 2 for supplying P_{Load} of the study site. All configurations are presented in Table 8, optimized under the capacity shortage at 0.0% and a Cycle Charging (CC) dispatch strategy to ensure uninterrupted power delivery.

Notably, System #1 Case 1 with architecture of PV/NIB/EL/FC/HSS comes up with the most techno-economic balanced solution. It is observed that NPC of \$1.53M and LCOE of 0.0649\$/kWh are the lowest among hydrogen integrated systems. Despite the additional cost of hydrogen infrastructure (EL, HTank and FC), the system has achieved 9% ROI and 11% IRR, which indicates strong financial viability. Therefore, this performance stems from effective utilization of hydrogen for seasonal energy shifting, enhancing reliability and reducing the BES burden and maintains 100% RE fractions with minimal excess energy (74.3%) implying good load-matching and storage synergy. in both cases.

In addition to this, Case 2 with architecture (PV/NIB without hydrogen) offers the NPC lowest \$1.30M and the LCOE to 0.0554 \$/kWh but maintains the RE fraction to 100%. But at the cost of 0% ROI and IRR are, which results in exceeding the payback period of project life. Therefore, it suggests that the cost reduction comes at the expense of financial sustainability. And the high excess energy (81%) also points to poor utilization of surplus energy generated by PV due to lack long-term storage (hydrogen).

Moving to System #2, which uses LIB's, and can be observes significantly higher capital and NPC values due to the higher cost and lower depth of discharge of LIBs. Such as Case 3 with architecture (PV/LIB with hydrogen) reaches NPC of \$2.35M with an LCOE of 0.1001\$/kWh making it financial unfeasible option. Despite having RE fraction of 99.6%, ROI of 6% and an IRR of 7%, with a 15-year simple payback period, which reduces its attractiveness. At last, the case 4 with hydrogen, reduces the NPC to \$2.26M but still results in negative ROI (-6%) and (0%) IRR, which indicates unsustainable financial. In contrast, the excess energy is again (~81%) in this case, which shows the curtailed renewables due to storage limitations.

Comparatively cross-case analysis reveals several insights:

- The NIBs consistently outperform economically than LIB, due to lower cost and higher round-trip efficiency.
- The integration of HSS improves energy utilization, ROI, and system autonomy, especially in NIB-based systems.
- Although excess energy is a function of both oversized PV capacity and limited storage capacity, therefore, hydrogen helps to absorb this surplus energy effectively.
- System #1 offers a better cost-benefit trade-off, balancing investment with return, while system #2 prioritizes higher RE penetration.

Therefore, this study analysed that the system #1 case 1 is identified as the most optimal configuration for an off-grid microgrid to meet the P_{Load}, Which provides significant cost reductions, higher ROI, and IRR, and ensures consistent 100% reliability, alongside offers the best blend of technical robustness, financial viability, and RE utilization, which makes it a sustainable model for off-gird electrification in rural Pakistan. However, further discussion and analysis are focused on this configuration due to its overall balanced performance.

Table 9
Summary of optimization at the capacity shortage of 0 % with a cycle charging dispatch strategy

Component	Unit	System #1		System #2	
		Case #1	Case #2	Case #3	Case #4
		PV/NIB/EL/FC /HSS	PV/NIB	PV/LIB/EL/ FC/HSS	PV/LIB
Solar PV	kW	2,834	2,834	2882	2,899
Fuel Cell	kW	250	N/A	250	N/A
Electrolyzer	kW	100	N/A	100	N/A
Hydrogen Tank	kg	100	N/A	100	N/A
BES	Quantity	1,658	1,658	2,615	2,104
Converter	kW	500	500	388	664
Economic Parameters					
NPC	$	1.53 M	1.30 M	2.36 M	2.26 M
LCOE	$/kWh	0.0649	0.0554	0.1001	0.0962
COH	$/kg	8.12	-	12.6	-
Return on investment (ROI)	%	9	0	6	-6
Internal rate of return (IRR)	%	11	0	7	0
Simple payback	year	9	>25	15	>25
Discounted payback	year	8.8	>25	14.9	>25
Electrical Parameters					
Annual electrical energy generation	kWh/year	49,23,300	49,23,300	50,40,363	50,36,554
Annual Solar PV generation	kWh/year	49,23,300	49,23,300	50,06,303	50,36,554
FC generation	kWh/year	34,165	-	34,059	-
Electrolyzer production	kg/year	7,075	-	7,052	-
Annual hydrogen gas consumption	kg/year	7,118.00	-	7,169	-
Annual throughput of BES	kWh/year	2,93,250	3,28,046	575	3,36,251
Autonomy hour from HTank	hour	33	-	33	-
Autonomy hour from BES	hour	32.5	33	34.3	33.3
RE fraction	%	100	100	100	100
Capacity shortage	%	0.0977	0.0988	0	0.0975
Unmet load	%	0.0494	0.0505	0	0.0487
Excess electrical energy generation	%	74.3	81	75	80.8

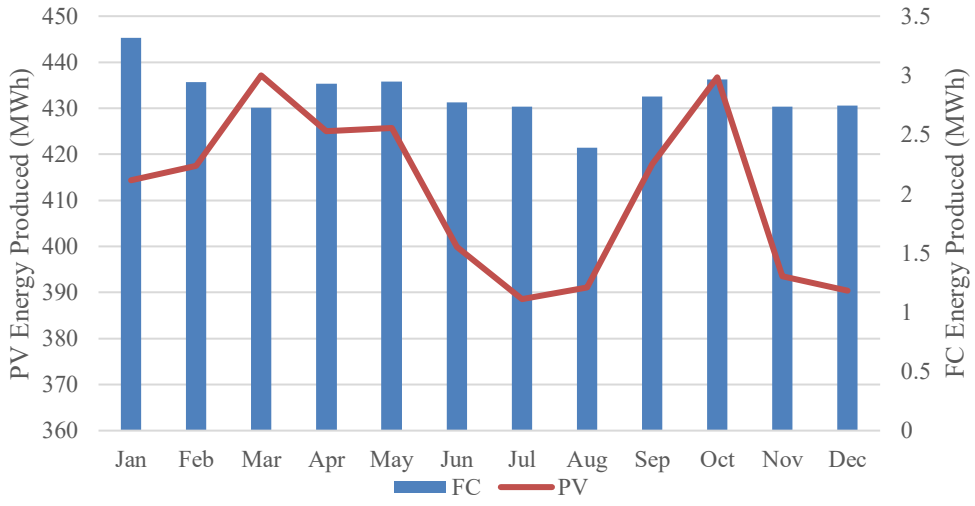

Fig 7. Monthly electrical energy generated.

4.2. Hybrid energy generation

The electrical energy generated monthly from system #1 case #1 is shown in Fig 7. It reveals the seasonal generation patterns, with the dominant energy source, which is solar PV, and contributes significantly throughout the year, where the seasonal variation is evident that the output peaking from March and August, due to high solar irradiance, and lower production is observed from November to February, aligning with regional climate data.

However, the fuel cell's contribution is lowest in summer season, but increase in low irradiance season, particularly January and December, reflecting its role as a supplementary during winter periods when the solar PV output is insufficient.

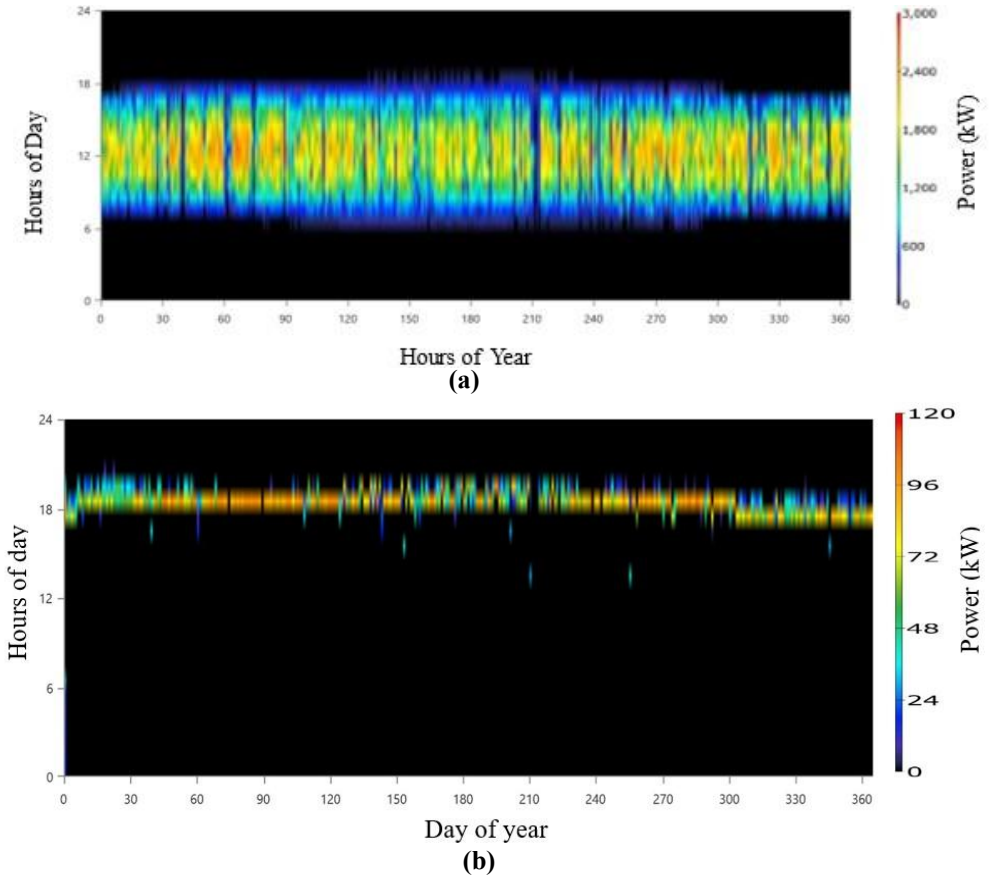

Fig 8. Annual output power, a) Solar PV and b) Fuel cell

This distribution pattern reflects the strategic use of hybrid design that leverages solar energy and hydrogen-based backup system to enhance system resilience during peak and off-peak solar periods, while ensuring year-round reliability. Solar PV generates maximum energy in the month of March to August, respectively, while the lowest generation occurs from January to March.

4.3. Solar PV and fuel cell generation

The electrical power produced per year from solar PV is shown in Fig 8(a). It reveals that the consistent PV operation over 4,735 hours/year, confirming its role as the base-load provider. The high annual energy yield of ~4.92 GWh, ensuring minimal unmet demand. Fig 8(b) reveals that the FC activity is limited to 554 hours/year, emphasizing its standby nature. Notably, 362 start-up events indicate frequent, short-term dispatches to full in power gaps, demonstrating fast response capability, on the contrary also pointing to possible degradation of risk as a result of frequent cycling.

The above discussion and data highlights that solar PV acts as the primary power source, however, the FC acts as a supplementary unit to ensure reliability during periods of insufficient solar generation.

4.4. Electrolyzer Input/Output

The EL yearly energy consumption, which peaks during the summer months (May-August), due to the excess availability of the solar power. It is, therefore, the system strategically diverts this surplus to the EL to produce hydrogen, thereby minimizing limitation and storing energy for later use. However, this utilization pattern ensures optimal system efficiency by converting the wasted energy into a valuable backup resource. As a result, lower energy consumption in winter corresponds with reduced PV output and direct load consumption, as shown in Fig. **9**(a).

Fig. **9**(b) reflects the trend in Figure 9(a), conforming that hydrogen production is directly related to surplus PV energy. However, the peak production in July aligns with the highest irradiance and lowest load-supply mismatch, and this hydrogen is used later in FC during low solar irradiance, primarily in winter. It is, therefore, the EL's specific energy consumption of 46.4 kWh/kg recommends a well-optimized operational schedule. The production of hydrogen is cyclic nature; therefore, it underlines the system's seasonal energy shifting capability, which enhance year-round reliability.

Fig. **9**(c) presents the monthly capacity factor of the EL, with values ranging from 30% to nearly 45%. These moderate capacity factors reflect the system's intentional part-load operation, driven by excess PV generation availability rather than round-the-clock use. High-capacity factors in June–August indicates efficient utilization of daytime solar surplus, while lower values in December–January align with diminished PV output. This reflects a smart energy management strategy, where the EL is run only when system conditions are optimal, maximizing hydrogen production efficiency while avoiding unnecessary wear. EL is used throughout the year to maintain the HTank level, which can be used in night-time or low I_h.

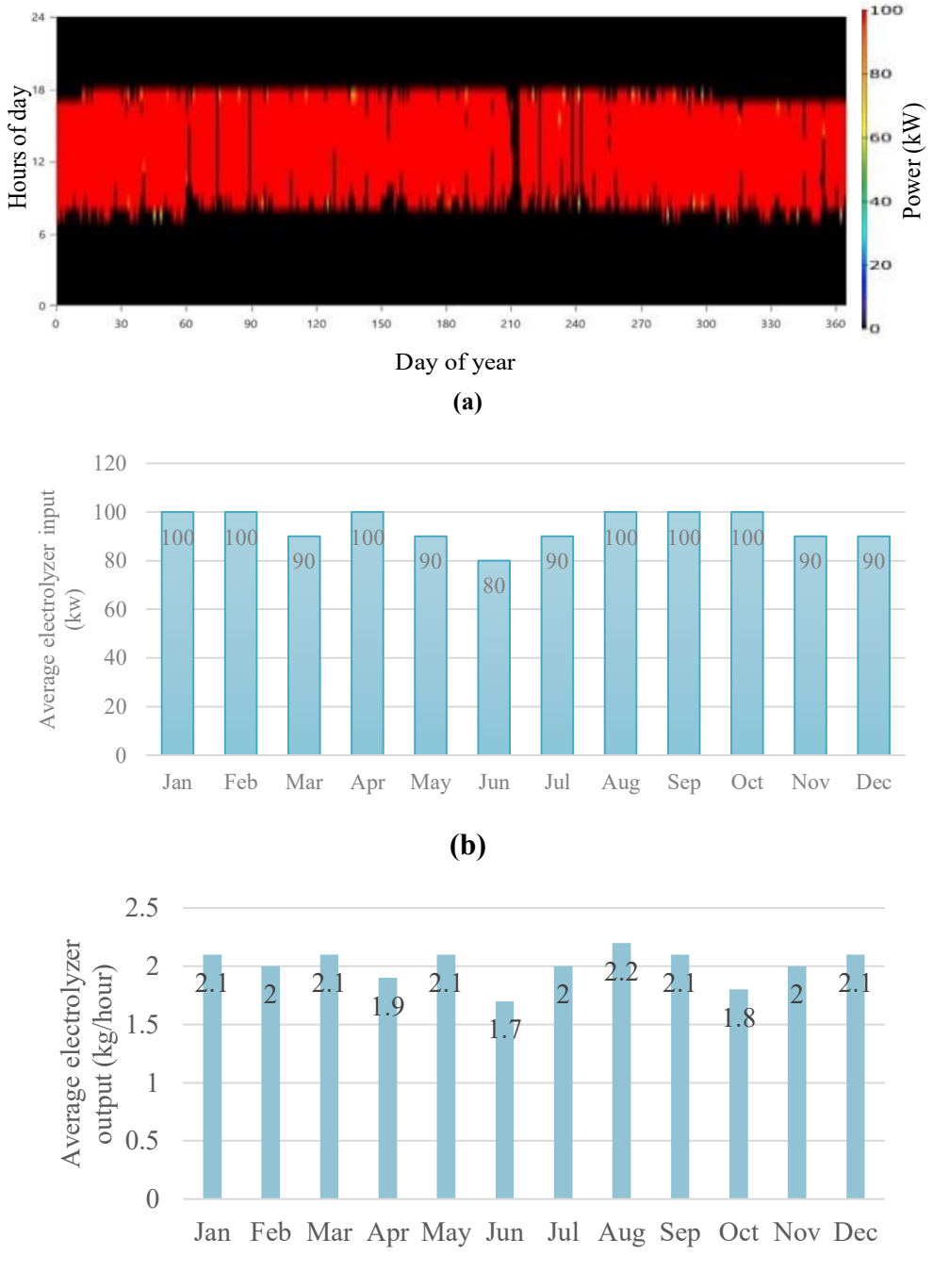

Fig. 9. Input power to the electrolyzer, (a) Yearly, (b) Monthly average, and (c) Monthly average output.

Figure 10 (a) illustrates the annual HTank's storage cycle, with levels peaking in mid-summer (July-August) and depleting within winter (December-January). Therefore, this seasonal pattern aligns with system's logic, which is store surplus solar energy in summer when irradiance is high, and use it in winter via the FC when solar production is low. However, it can be observed that HTank's plays a vital role in long-duration energy storage buffer, enabling energy shifting across months. The HSS has a maximum capacity of 100 kg, which can handle an autonomy of 33 hours to meet load demand. The variation of hydrogen volume in the HSS is presented, indicating levels that fluctuate between 0 and 50 kg, and the system's the system's design allows that full tank utilization without any overflows, therefore, indicating well-calibrated EL and tank sizing. The consumption patterns of stored hydrogen for electricity generation throughout the year is mostly at night and during cloudy periods, which demonstrates the effective integration of the HSS, and is illustrated in Figure 10 (b). Where, the total fuel consumption is 7,125 kg/year, with an average daily fuel consumption of 19.5 kg/day. However, it ensures that backup availability, facilitating consistent FC operations and reducing the risk of unmet load during intermittency.

During periods of excess energy generation, HTank effectively stores excess hydrogen, while consistently supplying fuel to the FC to ensure uninterrupted power supply during times of low I_h.

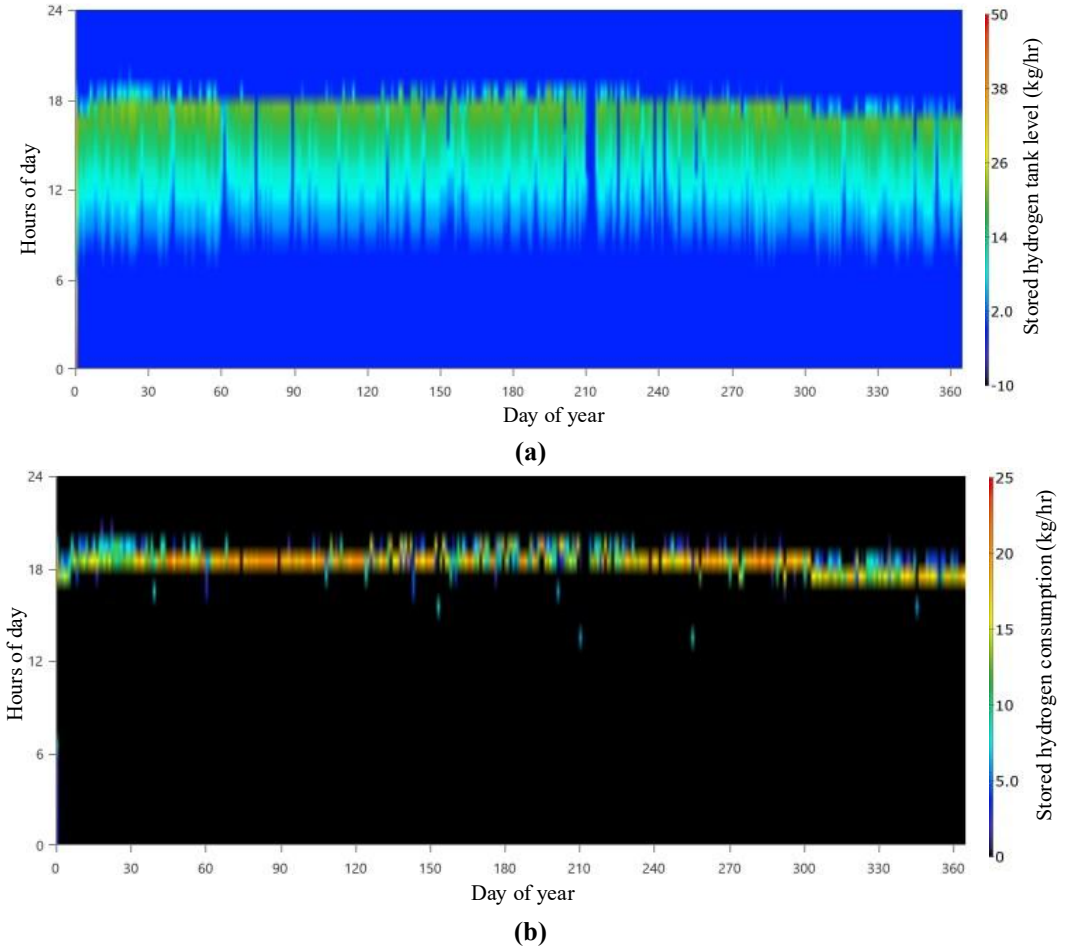

Figure 10. Annual, hydrogen (a) HTank level, (b) Stored/Consumption

The configuration system with EL and HSS types of equipment incorporate a consistent and efficient performance, ensuring reliable hydrogen production and availability for FC operation, as well as enhancing the resilience and autonomy of the proposed off-grid ESS.

4.5. State of charge (SOC) in BES

Fig 11 illustrates the daily SOC fluctuations profile of the BESS over a full operational year, with the consistently cycling between ~40% and 100%, which is mapped against hourly and daily resolutions. The heatmap visually represents the frequent high SOC levels indicates excess PV generation allowing near-full charging daily. In contrast, winter months (December-January) show shallower cycles, with the battery seldom fully charged, which confirm increased reliance on FC and reduced solar input. It is, therefore, the evaluation of storage utilization patterns, charging/discharging cycles, and overall system responsiveness to RE input and load demand fluctuations. However, statistically the BES received 300,181 kWh annually and delivered 285,586 kWh as output, and provides 32.5 hours of power during autonomy periods, with a yearly throughput of 293,005 kWh. Therefore, it is relatively stable SOC profile throughout the year, which reflects a well-sized battery bank and effectively load balancing, ensuring that energy is neither wasted nor in short supply.

It can be observed for the majority of year, the battery system maintains a high SOC, and indicates sufficient energy availability and optimal integration with solar generation. However, brief periods of low SOC, specifically noticeable

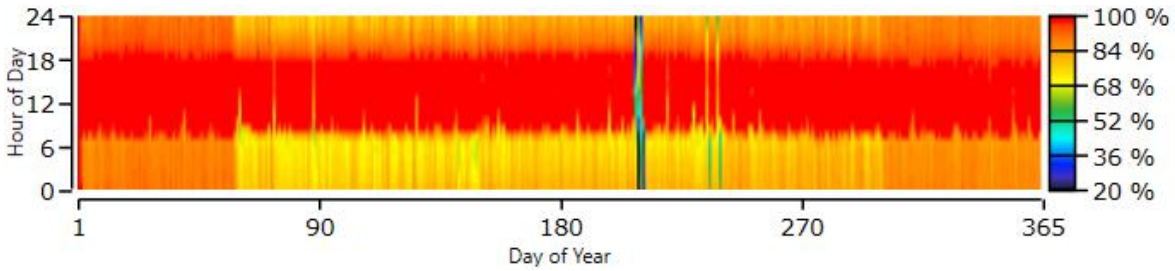

Fig 11. Annual state of charge of BES daily.

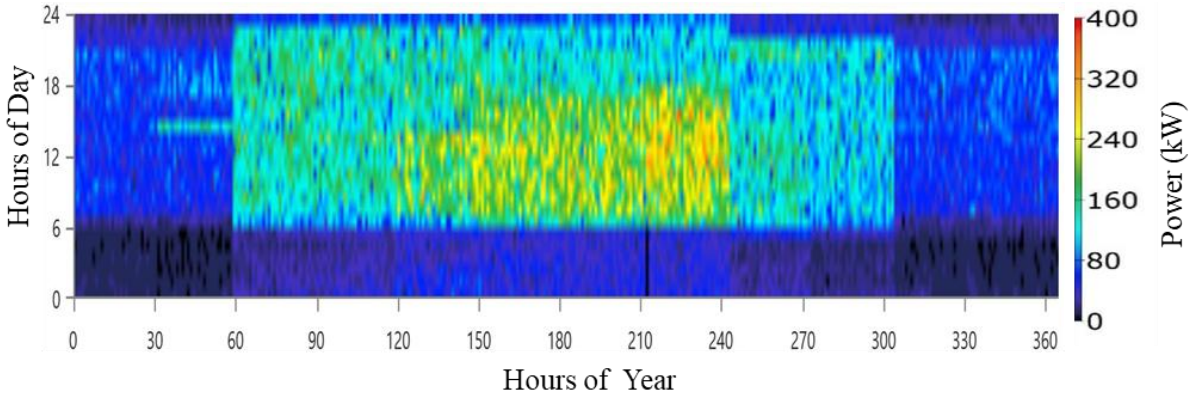

Fig 12. Converter output power as inverter.

around mid-year, and suggest high demand or low I_h, where auxiliary systems such as the FC or HSS may play an important role in ensuring energy balance and reliability.

4.6. Converter input/output

The monthly AC output of inverter, which reflects the overall energy consumption trend across the year, and to fulfil the requirements of the load demand, is illustrated in Fig 12. Which delivers the power to the EL and BES. The converter operates for a total of 8754 h/year, and the highest inverter output is recorded between May and August, with an energy input of 931,807 kWh/year and delivering 885,216 kWh/year as output, with energy losses of 46,590 kWh/year, respectively, with a capacity factor of 20.2%. It is driven by both high solar generation and increased community demand (e.g., cooling appliances). However, the drop-in inverter activity during December–January corresponds with reduced PV input and lower load levels. Therefore, this output profile reflects a well-sized inverter system that is neither underutilized nor overloaded, confirming its effective integration into the power delivery chain. Despite all facts, the system's ability to consistently convert DC power to AC for diverse loads, it demonstrates reliable and stable operation throughout the year, and ensures high-efficiency DC-AC power transformation.

Inverter activity increases during the mid-year period, corresponding with peak I_h and extended daylight hours, as a result, it maximizes energy supply to the AC load. On the other hand, the lower output observed during the early and late months, which indicates the low solar-PV generation, highlighting the inverter's dependence on PV input. It is, therefore, the dynamics highlight the critical role of the inverter, ensuring efficient energy conversion and providing an uninterrupted supply across fluctuating seasonal conditions.

4.7. Excess energy and unmet load

There are two key operational metrics in this session: monthly excess electricity and the RE fraction, Excess energy is generated by the proposed off-grid microgrid system when all load requirements are met, and is typically during May throughout the August, reaching value above 10% of monthly generation, as result, the storage systems are fully charged. However, this surplus generation arises due to high I_h, and relatively lower storage or load absorption at midday. Despite this, the RE fraction consistently remains at or near 100~ throughout the year, which highlights the system potential to operate entirely on RE sources without interference of fossil fuel backup. By highlighting the fact, that the capacity of the dump load depends on the amount of excess energy generated. H_2

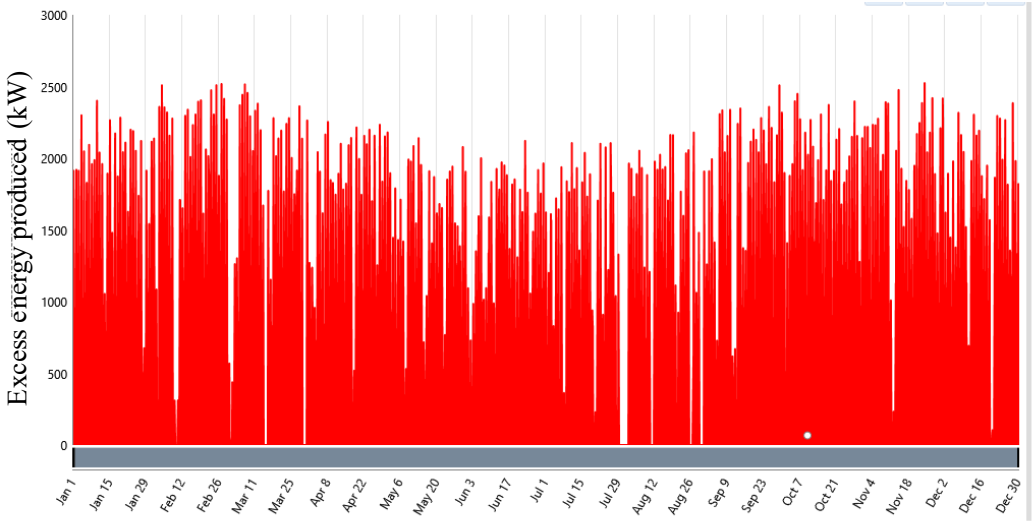

Fig 13. Excess energy produced at a capacity shortage of 0.0977 %.

Table 10
Emission analysis with Sodium-ion battery

Parameter	Component	Unit	System #1	
			Case #1	Case #2
			PV/NIB/FC/EL/HSS	PV/NIB
Emission	CO_2	Kg/year	-	-
	Carbon monoxide	Kg/year	1.43	-
	Sulfur dioxide	Kg/year	-	-
	Nitrogen Oxide	Kg/year	0.143	-

statistically, the yearly excess energy amounts to 74.3 % of the total energy generated, and the capacity shortage is 0.0977 %, where he maximum unmet load of 437 kWh/year, and the average annual unmet load is 0.0494 % at a capacity shortage of 0.0977 %. Therefore, it validates the fact that system's over-sizing strategy can ensures energy security even during worst-case scenarios of solar dips. Additionally, the potential opportunities for productive use applications, such as community cooling or water pumping, to absorb excess power and improve overall system performance along with utilization. This analysis emphasizes the importance of balanced generation and storage, ensuring operational reliability, efficient energy management, and minimal unmet load, which provides the system's capability to maintain stability in an off-grid microgrid system.

4.8. Emission analysis with Sodium-ion battery

The environmental impact of the two cases from system #1, is shown in Table 9. Which compares the emissions produced by two system configurations sing NIB: Case 1, includes hybrid system parameters (FC, EL, HSS), the hybrid system (PV/NIB/FC/EL/HSS), while case 2, is purely PV-based system. The difference in emissions underscore the environmental trade-offs between adding backup generation and relying only on renewables.

In case 1, small amounts of atmospheric pollutants (1.43 kg/year) of CO and (0.143 kg/year) of Nitric-Oxide (NO) with no Carbon Dioxide (CO_2) and SO_2 are emitted. However, these trace emissions originate from the operation of FC, which, although cleaner than fossil-fuel generators, still emits limited pollutants due to electrochemical reactions and auxiliary systems. Despite having hydrogen as subsystem, the system avoids CO_2 and Sulfur Dioxide (SO_2) emission, and this confirms that there are no carbon-based fuels or sulfur-containing materials are involved.

However, in case 2, only the use of the PV/NIB configuration, achieves complete zero-emission of all pollutants, including CO_2, CO, SO_2, and NO, are recorded as zero. This configuration operates entirely on electrochemical and PV principles, which produce neither gaseous nor particulate emission. And therefore, this makes it an ideal candidate for deployment in environmentally sensitive or emissions-regulated zones, especially where climate goals are a priority. However, the absence of backup hydrogen system in case 2 results in higher energy excess losses 81% and reduced energy autonomy, as seen in Table 8. Therefore, it achieves better environmental purity, but compromises energy resilience and economic return.

Despite, the integration of HSS and FCs, which can slightly effects emission profile but still remains carbon-free and dramatically cleaner than conventional diesel or fossil-fuel based microgrids. It is important to note that the key is to find the right balance between ultra-low emissions and functional energy security, which is effectively demonstrated by case 1 of System #1.

4.9. Economics analysis

Fig 14 provides a detailed cost breakdown of System #1 (Case 1), segmented by component across different cost categories: capital, operating, replacement, and salvage.

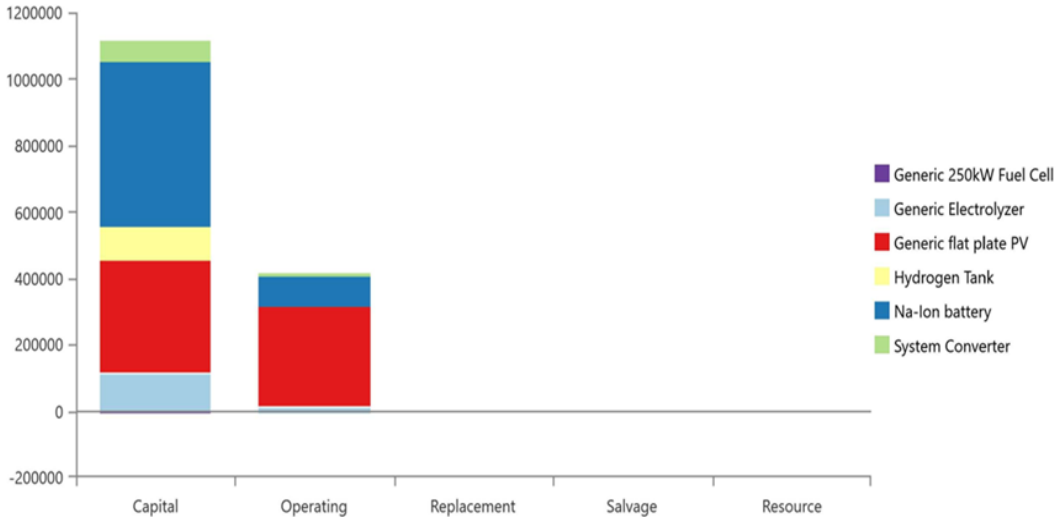

Fig 14. Cost summary

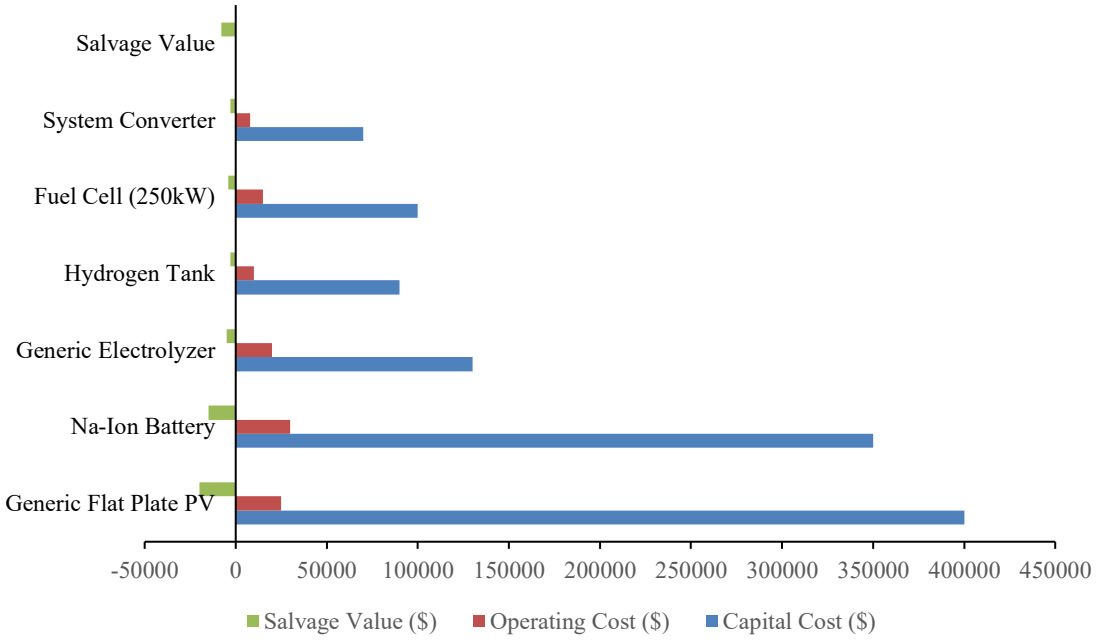

Fig 15. Cash flow of cost, and system component-wise.

The capital cost is dominated by the Na-Ion battery (blue) and generic flat plate PV modules (red), together contributing over 70% of initial investment. The EL (light blue) and hydrogen tank (yellow) also represent notable shares, confirming the additional cost burden of integrating long-duration hydrogen storage.

On the operating cost side, the battery again appears significant, reflecting maintenance and system management requirements, followed by moderate contributions from the PV and EL subsystems. Interestingly, replacement costs appear to be negligible in this figure, which suggests that either the components' life exceeds the project duration, or the costs were absorbed upfront—this should be clarified in the simulation model or results section.

Salvage values (negative costs) are visible but minor, mostly contributed by the fuel cell and PV system, indicating end-of-life residual value. The stacked bar format reveals the relative contribution of each component, helping identify areas where future cost optimization (e.g., in battery or hydrogen subsystems) could significantly impact overall project economics.

This indicates that the NIB system has the highest capital costs, followed by, solar PV, EL, FC, and converter. The highest operating cost is required for Solar PV, followed by NIB, converter, and FC. The replacement cost of NIB is $99262, respectively. Similarly, the salvage value at the end of the project lifetime received from the NIB and FC is $51076 and $2039, respectively. Fig 15 shows the annual cash flow in different cost components of the proposed system over a 25-year project lifespan, including capital cost, O&M, and salvage value. The total capital investment is $274042. Similarly, total O&M and replacement costs are $118695 and $99262. The major capital investment occurs at year 0, while recurring replacement and O&M costs appear in regular intervals, notably for batteries (~Year 10) and inverters (~Years 15). However, the annual cost recovery through avoided diesel fuel and grid extension cost enables a consistent economic return, which leads to payback in year 9.

However, the total system cost into capital, replacement, O&M, and salvage, and the Capital cost dominates the overall cost, and is accounting for nearly 60% of total investment, primarily due to PV modules, HSS, BES and FC, which is the constitute of the next significant portion. Relatively the O&M cost are modest, reflecting the-maintenance nature of RE system. At last, the salvage value is recovered but it is important to address the cash flow according to the system components in various years until the project is completed.

In summary, the presented cost-distribution charts effectively elucidate the financial contributions of each system component by juxtaposing capital, operating, and replacement expenditures on a uniform axis. The grouped-bar format mitigates the visual dominance of high-magnitude elements, such as the NIB and flat-plate PV, thereby facilitating direct comparison with lower-cost components like the EL and converter. This balanced visualization underscores the disproportionate allocation of capital investment toward battery storage and PV generation, however, highlighting the non-negligible operating expenses associated with these assets. Such clarity in cost breakdown is essential for informed decision-making in off-grid microgrid design, enabling stakeholders to target cost-optimization strategies where they will yield the greatest impact.

4.10. Economic analysis with sodium-ion battery

Table 10 shows the economic performance of the NIB compared with the two NIB-based configurations, case 1, which includes hydrogen components, and case 2, purely PV/NIB system. However, the comparison highlights a clear trade-off between initial affordability and long-term financial viability.

Table 11
Economic analysis with NIB

Parameter	Component	Unit	System #1	
			Case #1 PV/NIB/FC/EL/HSS	Case #2 PV/NIB
System Architecture	Solar PV	kW	2834	2834
	Fuel Cell	kW	250	-
	Electrolyzer	kW	100	-
	Hydrogen Tank	kg	100	-
	BES	Quantity	1658	1658
	Converter	kW	500	500
	Fuel	kg	7,175	-
Cost	NPC	$	1.53 M	1.30 M
	CAPEX	$	1.15 M	0.90 M
	OPEX	$/year	15583	15154
	LCOE	$/kWh	0.0649	0.0554
	COH	$/kg	8.12	-
	ROI	%	9	0
	IRR	%	11	0
	Simple payback period	year	9	>25

In the economic analysis, case 2 demonstrates the most cost-effective metrics, with the lowest NPC $1.30 M, Initial Capital Cost (ICC) $0.9M, and the LCOE 0.0554 $/kWh. Therefore, this makes it attractive or institution with tight upfront funding constraints. However, the model shows no return on investment (ROI = 0%) and payback period is exceeding the project life horizon of 25-year, which indicates that the financial savings generated are insufficient to recover the investment during the lifecycle of systems. As a result, it reflects a low risk-low return model, which is sustainable mainly when cost minimization dominates financial profitability.

In Addition, case 1, though more expensive upfront with a NPC of $1.53M, a Capital Expenditure (CAPEX) of $1.15M, and LCOE of $0.0649/kWh, which offers much stronger long-term financial performance. However, it yields a 11% IRR, 9% ROI, and a payback period of just 9 years, making it economically sustainable over the full lifecycle, and this improvement stems from better energy flexibility, reduced limitations, and hydrogen-based energy shifting that enhances system potential. The fuel Cost of Hydrogen (COH) is $8.12/kg relatively competitive for off-gird settings, especially given the 7,175 kg/year of fuel use, which helps to reduce reliance on oversized batteries.

Despite the higher initial investment and operating costs, reflects added maintenance and replacement needs for hydrogen components, but these are offset by financial returns. This case 1 offers a more aligned with resilient rural electrification programs or mini-grid operators seeking long-term autonomy of energy and return on capital investment.

This study presents two different cases, which offer valuable insights into the economic and operational aspects of an energy, by ensuring both technical viability and economic feasibility. Therefore, the results suggest that case 2 is ideal for cost-sensitive, short-term deployment, and is the most economically favorable, with the lowest NPC, ICC, and LCOE. However, case 1 offers more balanced and future-proof approach, with comprehensive energy generation capabilities, and provides trades off higher CAPEX for improved financial and operational outcomes, which might be beneficial for long-term sustainability. Both cases provide their respective advantages, depending on the operational properties and financial goals of the project.

4.11 Comparative analysis

Table 11 presents a comparison of HRES in various countries from a range of recent studies, focusing on system configurations, including the system components used (PV, WT, DG, FCs, BESS, Battery Management System (BMS), and converters, with economic constraints, including Total NPC (TNPC) and Cost of Energy (COE). However, the intent is to benchmark the current study's configuration against international designs in terms of cost-effectiveness, technical feasibility, economic viability, and energy architecture.

Notably, the novel system proposed in this research is distinct due to achieving the lowest LCOE of 0.0649/kWh among all cases, able it with a comparatively higher NPC of 0.0649$/kWh among all cases, able it with a comparatively higher NPC of $1.53 M. This is caused by the refined strategic interplay between the capital expenditure and performance parameters of the system, especially with the inclusion of Na-ion batteries and hydrogen storage. Their emerging battery technology (NIB) adoption unlike other studies with Li-ion or diesel systems not only sustains the system's 100% renewable fraction and autonomy but also reduces lifecycle costs.

Conversely, in their work, Dash et al. (2023) and Hasan et al. (2023) report LCOE values of 0.18 and 0.12 $/kWh respectively. While their configurations seem somewhat PV-Wind-Battery and Solar-Wind-HSS hybrid, these values indicate higher costs driven by less optimized dispatch strategies, higher component pricing, or limited energy storage integration. Zhang et al. (2019) and Li et al. (2020), who incorporate hydrogen, also showcase a lack of cost-efficient design, which points to the influence of system sizing and battery choice on efficiency.

Furthermore, the previous research focuses on the very specific targets such as diesel reduction, urban microgrids or peak shaving. Therefore, this study at hand has a focus cantered to unreliably-grid connected rural areas, by emphasizing energy autonomy and reliability.

This study incorporates a slightly higher NPC due to the size of the off-grid microgrid system, compared to

Table 12
Sensitivity Analysis Summary

Parameter	% Variation			
	-2%	+2%	LCOE Range ($/kWh)	NPC Variation
Discount Rate	6%	10%	0.058 – 0.072	±9%
Inflation Rate	5%	9%	0.061 – 0.070	±6%
PV CAPEX	-20%	20%	0.060 – 0.072	±11%
Load Scenarios	80%	120%	0.060 – 0.073	±15%

contemporary literature. However, it can be further reduced by incorporating the size of the system. Therefore, this study achieve ~41.8% lower LCOE than the average LCOE in comparable to previous studies and can be further reduced depending on the load demand and system requirements, which ensures scalability of the system.

4.12. Sensitivity Analysis

To analyse the system's performance and model robustness towards the different input parameters. The sensitivity analysis was performed for system #1 case #1 on techno-economic parameters. To ensure the robustness of the model and economic assumptions were taken. The three load scenarios with economic parameters were simulated, and a summary of the sensitivity analysis is shown in Table 12. As a results, it impacts on various financial factors of the economic feasibility for the whole system. Some of the important parameters that were evaluated for the purpose of this study were discount rates, inflation rates, and capital expenditure for both photovoltaic CAPEX.

However, all these factors contribute moderately towards LCOE and NPC of the system, whether it is an increase or decrease, i.e., decreasing the discount rate to 6% results in a LCOE decrease to 0.058 $/kWh. On the other hand, increasing the discount rate will increase LCOE to 0.078 $/kWh, resulting in a ±9% change in NPC. It is, therefore, shifts in the inflation rate led to LCOE oscillations between 0.061 and 0.070 $/kWh, resulting in NPC fluctuation of ±6%. In terms of economic sensitivity, increases in LCOE or NPC due to 20% increases in PV CAPEX will lead to 0.072 $/kWh. On the other hand, a reduction of 20% results in NPC of 0.060 $/kWh. These results indicate a clear trend with regard to sensitivity of the economic assumptions made with regards to cost projections being more controlled.

4.13. Grid Extension Feasibility

The economic feasibility of electrification via extending the grid to sparsely populated or remote areas like Ruk village is challenging despite being technically possible. The infrastructure cost for rural grid extension in Pakistan is reported to be 15,000 to 25,000 per km based on access and terrain considerations (ADB, 2021; NEPRA, 2023). Assuming an 18 km distance extension from the nearest substation, the proposed cost would range from $270,000 to $450,000. However, grid extension costs vary by region, distance, and load density. The following benchmarks contextualize costs for Ruk, located 18 km from the nearest grid node, given as follows:

- Pakistan: The estimate rural grid extension costs at $15,000–$25,000/km. For an 18-km line to serve 172 households (145.61 kW peak load), the capital cost is $270,000–$450,000, excluding distribution equipment ($50,000–$100,000 for transformers and substations) and annual maintenance ($5,000–$10,000/km/year, totalling $90,000–$180,000 over 25 years) (ADB, 2018; NEPRA, 2020).
- Bangladesh: Grid extension LCOE ranging from $0.16/kWh (1 km) to $1.65/kWh (25 km) for loads of 5–50 kW, driven by reduced load density and technical losses (15–20%) (Islam et al., 2022).

For this study especially for village Ruk's 145.61 kW load, LCOE is estimated at $0.20–$0.50/kWh for 18 km, aligning with Pakistan's cost profile. Therefore, these benchmarks highlight the high capital and operational costs of grid extension, particularly for remote, low-density areas.

In addition, problems like poor long-distance voltage regulation, frequent blackouts, and elevated technical losses per distance severely hinder the long-span rural grid extensions. Add to this the ongoing costs of maintenance for the extended transmission systems, and centralized grid solutions become less practical. Consequently, off grid solutions appear more reliable alongside economically viable options.

5. Conclusion and recommendations

5.1. Conclusion

This study presents the simulation results of an off-grid microgrid system powered by PV, FC, EL, and BES with Na-ion battery technology. The system configurations were simulated using HOMER Pro software to meet the energy demands of a rural community. The total yearly electrical energy production from PV and FC, along with the economic and environmental impact, were evaluated. Based on the analysis of two cases, it is evident that both configurations can meet the energy demand with 100% RE sources. However, a detailed economic assessment reveals important differences in performance.

To assess the system configurations, key economic indicators were used: total NPC, CAPEX, Operating Cost (OPEX), and LCOE. The configuration with PV, FC, EL, HSS, and BES (case #1) emerged as the most comprehensive solution, offering higher energy generation capabilities and an LCOE of $0.0649/kWh. This system has an NPC of $1.53 million and achieved a RE fraction of 99.3%. The configuration with PV and BES only (case #2) demonstrated a lower NPC of $1.30 million and a reduced LCOE of $0.0554/kWh, making it the most cost-effective option. This system also achieved a 100% RE fraction with no unmet load or emissions.

In terms of emissions, the hybrid system (case #1) produced small amounts of pollutants, including 1.43 kg/year of CO and 0.143 kg/year of NOx, while the PV/BES-only system (case #2) resulted in zero emissions, indicating a completely clean energy system.

Comparative analysis between the configurations highlights distinct advantages. The hybrid system with FC, EL, and HSS offers better energy generation and reliability, while the simpler PV/BES system proves to be more

economically favorable. Future work could explore additional configurations, including the integration of hydrogen storage and demand-side management strategies, to further optimize system performance. This study provides valuable insights into the design and optimization of energy systems for rural electrification, offering stakeholders practical solutions for achieving energy independence and sustainability. The findings contribute to ongoing efforts to reduce reliance on fossil fuels and minimize the environmental impact of rural energy systems.

5.2. Recommendation

This research paper provides two perspectives for the consumers, that the economic and technical variables need to be analysed to determine the optimal system in the case of these two systems. System #1 has better economic results compared to system #2 because it has a lower NPC and LCOE, that makes it more economical. System #2 has better technical performance with a higher RE fraction and better capacity utilization, so all parameters of its effectiveness and reliability are improved. The selection of the systems is purely a question of demand. Cost minimization or reduction of technical performance system reliability is the only focus. It is therefore, the definition of the more appropriate system choice should be consistent with the needs and goals from the consumer's perspective, one with more economic and technical constraints as well as long-term sustainability.

Acknowledgement

The authors would like to acknowledge Mehran University of Engineering and Technology Jamshoro.

References

Abd El-Sattar, H., Kamel, S., Sultan, H. M., Zawbaa, H. M., & Jurado, F. (2022). Optimal design of photovoltaic, biomass, fuel cell, hydrogen tank units and electrolyzer hybrid system for a remote area in Egypt. *Energy Reports*, *8*, 9506-9527. https://doi.org/10.1016/j.egyr.2022.07.060

Abdin, Z., & Mérida, W. (2019). Hybrid energy systems for off-grid power supply and hydrogen production based on renewable energy: A techno-economic analysis. *Energy Conversion and management*, *196*, 1068-1079. https://doi.org/10.1016/j.enconman.2019.06.068

ADB. (2018). *Asian Development Bank Annual Report 2018*. https://www.adb.org/documents/adb-annual-report-2018

ADB. (2021). *Asian Development Bank Annual Report 2021*. https://www.adb.org/documents/adb-annual-report-2021

Ahmed, K. S., & Karthikeyan, S. P. (2018). Modified penalized quoted cost method for transmission loss allocation including reactive power demand in deregulated electricity market. *Sustainable Energy, Grids and Networks*, *16*, 370-379. https://doi.org/10.1016/j.segan.2018.10.004

Al-Sharafi, A., Sahin, A. Z., Ayar, T., & Yilbas, B. S. (2017). Techno-economic analysis and optimization of solar and wind energy systems for power generation and hydrogen production in Saudi Arabia. *Renewable and Sustainable Energy Reviews*, *69*, 33-49. https://doi.org/10.1016/j.rser.2016.11.157

Alam, M., Kumar, K., & Dutta, V. (2021). Design and economic evaluation of low voltage DC microgrid based on hydrogen storage. *International Journal of Green Energy*, *18*(1), 66-79. https://doi.org/10.1080/15435075.2020.1831506

Askarzadeh, A., & dos Santos Coelho, L. (2015). A novel framework for optimization of a grid independent hybrid renewable energy system: A case study of Iran. *Solar Energy*, *112*, 383-396. https://doi.org/10.1016/j.solener.2014.12.013

Ayeng'o, S. P., Schirmer, T., Kairies, K.-P., Axelsen, H., & Sauer, D. U. (2018). Comparison of off-grid power supply systems using lead-acid and lithium-ion batteries. *Solar Energy*, *162*, 140-152. https://doi.org/10.1016/j.solener.2017.12.049

Ayodele, T. R., Jimoh, A., Munda, J. L., & Agee, J. T. (2014). Viability and economic analysis of wind energy resource for power generation in Johannesburg, South Africa. *International Journal of Sustainable Energy*, *33*(2), 284-303. https://doi.org/10.1080/14786451.2012.762777

Aziz, A. S., Tajuddin, M. F. N., Adzman, M. R., Azmi, A., & Ramli, M. A. (2019). Optimization and sensitivity analysis of standalone hybrid energy systems for rural electrification: A case study of Iraq. *Renewable energy*, *138*, 775-792. https://doi.org/10.1016/j.renene.2019.02.004

Babatunde, O., Munda, J., & Hamam, Y. (2022). Off-grid hybrid photovoltaic–micro wind turbine renewable energy system with hydrogen and battery storage: Effects of sun tracking technologies. *Energy conversion and management*, *255*, 115335. https://doi.org/10.1016/j.enconman.2022.115335

Bakhtiari, H., & Naghizadeh, R. A. (2018). Multi-criteria optimal sizing of hybrid renewable energy systems including wind, photovoltaic, battery, and hydrogen storage with ε-constraint method. *IET renewable power generation*, *12*(8), 883-892. https://doi.org/10.1049/iet-rpg.2017.0706

Belkhiria, S., Briki, C., Dhaou, M. H., Sdiri, N., Jemni, A., Askri, F., & Nasrallah, S. B. (2017). Experimental study of metal–hydrogen reactor behavior during desorption under heating by electromagnetic induction. *International journal of hydrogen Energy*, *42*(26), 16645-16656. https://doi.org/10.1016/j.ijhydene.2017.04.295

Boglou, V., Karavas, C. S., Karlis, A., & Arvanitis, K. (2022). An intelligent decentralized energy management strategy for the optimal electric vehicles' charging in low-voltage islanded microgrids. *International Journal of Energy Research*, *46*(3), 2988-3016. https://doi.org/https://doi.org/10.1002/er.7358

Chauhan, A., & Saini, R. (2016). Techno-economic optimization based approach for energy management of a stand-alone integrated renewable energy system for remote areas of India. *Energy*, *94*, 138-156. https://doi.org/10.1016/j.energy.2015.10.136

Dargahi, A., Ploix, S., Soroudi, A., & Wurtz, F. (2014). Optimal household energy management using V2H flexibilities. *COMPEL: The International Journal for Computation and Mathematics in Electrical and Electronic Engineering*, *33*(3), 777-792. https://doi.org/10.1108/COMPEL-10-2012-0223

Das, M., Singh, M. A. K., & Biswas, A. (2019). Techno-economic optimization of an off-grid hybrid renewable energy system using metaheuristic optimization approaches–case of a radio transmitter station in India. *Energy conversion and management*, *185*, 339-352. https://doi.org/10.1016/j.enconman.2019.01.107

Dash, R. L., Mohanty, B., & Hota, P. K. (2023). Energy, economic and environmental (3E) evaluation of a hybrid wind/biodiesel generator/tidal energy system using different energy storage devices for sustainable power supply to an Indian archipelago. *Renewable Energy Focus*, *44*, 357-372. https://doi.org/10.1016/j.ref.2023.01.004

El-Sattar, H. A., Kamel, S., Sultan, H. M., Zawbaa, H., & Jurado, F. (2022). Optimal design of photovoltaic, biomass, fuel cell, hydrogen tank units and electrolyzer hybrid system for a remote area in Egypt. *Energy Reports*, 8, 9506-9527. https://doi.org/10.1016/j.egyr.2022.07.060

El Fathi, A., & Outzourhit, A. (2018). Technico-economic assessment of a lead-acid battery bank for standalone photovoltaic power plant. *Journal of Energy Storage*, *19*, 185-191. https://doi.org/10.1016/j.est.2018.07.019

Farinis, G. K., & Kanellos, F. D. (2021). Integrated energy management system for Microgrids of building prosumers. *Electric Power Systems Research*, *198*, 107357. https://doi.org/10.1016/j.epsr.2021.107357

Fodhil, F., Hamidat, A., & Nadjemi, O. (2019). Potential, optimization and sensitivity analysis of photovoltaic-diesel-battery hybrid energy

system for rural electrification in Algeria. *Energy*, *169*, 613-624. https://doi.org/10.1016/j.energy.2018.12.049

Gebrehiwot, K., Mondal, M. A. H., Ringler, C., & Gebremeskel, A. G. (2019). Optimization and cost-benefit assessment of hybrid power systems for off-grid rural electrification in Ethiopia. *Energy*, *177*, 234-246. https://doi.org/10.1016/j.energy.2019.04.095

Gharavi, H., Ardehali, M., & Ghanbari-Tichi, S. (2015). Imperial competitive algorithm optimization of fuzzy multi-objective design of a hybrid green power system with considerations for economics, reliability, and environmental emissions. *Renewable energy*, *78*, 427-437. https://doi.org/10.1016/j.renene.2015.01.029

Ghorbani, N., Kasaeian, A., Toopshekan, A., Bahrami, L., & Maghami, A. (2018). Optimizing a hybrid wind-PV-battery system using GA-PSO and MOPSO for reducing cost and increasing reliability. *Energy*, *154*, 581-591. https://doi.org/10.1016/j.energy.2017.12.057

Hasan, T., Emami, K., Shah, R., Hassan, N., Belokoskov, V., & Ly, M. (2023). Techno-economic assessment of a hydrogen-based islanded microgrid in north-east. *Energy Reports*, *9*, 3380-3396. https://doi.org/10.3390/en11040757

Hussain Mirjat, N., Uqaili, M. A., Harijan, K., Mustafa, M. W., Rahman, M. M., & Khan, M. W. A. (2018). Multi-criteria analysis of electricity generation scenarios for sustainable energy planning in Pakistan. *Energies*, *11*(4), 757. https://doi.org/10.3390/en11040757

IEA. (2024). International Energy Agency. *approximately 760 million people worldwide still lack access to electricity, with a significant proportion residing in rural communities* https://www.iea.org/reports/world-energy-outlook-2024

Ishraque, M. F., Shezan, S. A., Ali, M., & Rashid, M. (2021). Optimization of load dispatch strategies for an islanded microgrid connected with renewable energy sources. *Applied Energy*, *292*, 116879. https://doi.org/10.1016/j.apenergy.2021.116879

Islam, M. R., Akter, H., Howlader, H. O. R., & Senjyu, T. (2022). Optimal sizing and techno-economic analysis of grid-independent hybrid energy system for sustained rural electrification in developing countries: A case study in Bangladesh. *Energies*, *15*(17), 6381. https://doi.org/10.3390/en15176381

Jahannoosh, M., Nowdeh, S. A., Naderipour, A., Kamyab, H., Davoudkhani, I. F., & Klemeš, J. J. (2021). New hybrid meta-heuristic algorithm for reliable and cost-effective designing of photovoltaic/wind/fuel cell energy system considering load interruption probability. *Journal of Cleaner Production*, *278*, 123406. https://doi.org/10.1016/j.jclepro.2020.123406

Jahannoush, M., & Nowdeh, S. A. (2020). Optimal designing and management of a stand-alone hybrid energy system using meta-heuristic improved sine–cosine algorithm for Recreational Center, case study for Iran country. *Applied Soft Computing*, *96*, 106611. https://doi.org/10.1016/j.asoc.2020.106611

Jiang, J., Zhou, R., Xu, H., Wang, H., Wu, P., Wang, Z., & Li, J. (2022). Optimal sizing, operation strategy and case study of a grid-connected solid oxide fuel cell microgrid. *Applied Energy*, *307*, 118214. https://doi.org/10.1016/j.apenergy.2021.118214

Justo, J. J., Mwasilu, F., Lee, J., & Jung, J.-W. (2013). AC-microgrids versus DC-microgrids with distributed energy resources: A review. *Renewable and Sustainable Energy Reviews*, *24*, 387-405. https://doi.org/10.1016/j.rser.2013.03.067

Kaabeche, A., & Bakelli, Y. (2019). Renewable hybrid system size optimization considering various electrochemical energy storage technologies. *Energy conversion and management*, *193*, 162-175. https://doi.org/10.1016/j.enconman.2019.04.064

Kamran, M., Asghar, R., Mudassar, M., Ahmed, S. R., Fazal, M. R., Abid, M. I., Asghar, M. U., & Zameer, M. Z. (2018). Designing and optimization of stand-alone hybrid renewable energy system for rural areas of Punjab, Pakistan. *Int. J. Renew. Energy Res*, *8*(4), 2385-2397. https://www.ijrer.com/index.php/ijrer/article/view/14003

Kapen, P. T., Nouadje, B. A. M., Chegnimonhan, V., Tchuen, G., & Tchinda, R. (2022). Techno-economic feasibility of a PV/battery/fuel cell/electrolyzer/biogas hybrid system for energy and hydrogen production in the far north region of cameroon by using HOMER pro. *Energy Strategy Reviews*, *44*, 100988. (https://doi.org/10.1016/j.esr.2022.100988)

Khan, N., Dilshad, S., Khalid, R., Kalair, A. R., & Abas, N. (2019). Review of energy storage and transportation of energy. *Energy Storage*, *1*(3), e49. https://doi.org/10.1002/est2.49

Khatri, S. A., Mirjat, N. H., Harijan, K., Uqaili, M. A., Shah, S. F., Shaikh, P. H., & Kumar, L. (2022). An overview of the current energy situation of Pakistan and the way forward towards green energy implementation. *Energies*, *16*(1), 423. https://doi.org/10.3390/en16010423

Kim, H., & Jung, T. Y. (2018). Independent solar photovoltaic with Energy Storage Systems (ESS) for rural electrification in Myanmar. *Renewable and Sustainable Energy Reviews*, *82*, 1187-1194. https://doi.org/10.1016/j.rser.2017.09.037

Kitson, J., Williamson, S. J., Harper, P., McMahon, C., Rosenberg, G., Tierney, M., Bell, K., & Gautam, B. (2018). Modelling of an expandable, reconfigurable, renewable DC microgrid for off-grid communities. *Energy*, *160*, 142-153. https://doi.org/10.1016/j.energy.2018.06.219

Konneh, K. V., Adewuyi, O. B., Gamil, M. M., Fazli, A. M., & Senjyu, T. (2023). A scenario-based multi-attribute decision making approach for optimal design of a hybrid off-grid system. *Energy*, *265*, 125663. https://doi.org/10.1016/j.energy.2022.125663

Kumar, K., Alam, M., Rakshit, D., & Dutta, V. (2019). Operational characteristics of metal hydride energy storage system in microgrid. *Energy conversion and management*, *187*, 176-190. https://doi.org/10.1016/j.enconman.2019.03.019

Kumar, K., Alam, M., Verma, S., & Dutta, V. (2020). Analysis of metal hydride storage on the basis of thermophysical properties and its application in microgrid. *Energy conversion and management*, *222*, 113217. https://doi.org/10.1016/j.enconman.2020.113217

Kumar, K., Srivastava, J., Rakshit, D., & Dutta, V. (2017). Performance characterization of zero carbon emission microgrid in subtropical climate based on experimental energy and exergy analyses. *Energy conversion and management*, *154*, 224-243. https://doi.org/10.1016/j.enconman.2017.10.044

Kumar, P., Pal, N., & Sharma, H. (2022). Optimization and techno-economic analysis of a solar photo-voltaic/biomass/diesel/battery hybrid off-grid power generation system for rural remote electrification in eastern India. *Energy*, *247*, 123560. https://doi.org/10.1016/j.energy.2022.123560

Li, C., Zhou, D., Wang, H., Lu, Y., & Li, D. (2020). Techno-economic performance study of stand-alone wind/diesel/battery hybrid system with different battery technologies in the cold region of China. *Energy*, *192*, 116702. https://doi.org/10.1016/j.energy.2019.116702

Luta, D. N., & Raji, A. K. (2018). Decision-making between a grid extension and a rural renewable off-grid system with hydrogen generation. *International journal of hydrogen Energy*, *43*(20), 9535-9548. https://doi.org/10.1016/j.ijhydene.2018.04.032

Luthander, R., Lingfors, D., Munkhammar, J., & Widén, J. (2015). Self-consumption enhancement of residential photovoltaics with battery storage and electric vehicles in communities. *Proceedings of the ECEEE Summer Study on Energy Efficiency, Hyères, France*, *11*. https://doi.org/10.1016/j.energy.2016.06.039

Ma, H., Zhang, Y., Sun, S., Liu, T., & Shan, Y. (2023). A comprehensive survey on NSGA-II for multi-objective optimization and applications. *Artificial Intelligence Review*, *56*(12), 15217-15270. https://doi.org/10.1007/s10462-023-10526-z

Manoo, M. U., Shaikh, F., Kumar, L., & Arıcı, M. (2024). Comparative techno-economic analysis of various stand-alone and grid connected (solar/wind/fuel cell) renewable energy systems. *International journal of hydrogen Energy*, *52*, 397-414. https://doi.org/10.1016/j.ijhydene.2023.05.258

Mariama, S. M., Scipioni, A., Davat, B., & El Ganaoui, M. (2018). The idea of feeding a rural area in Comoros with a micro-grid system with renewable energy source with hydrogen storages. 2018 6th International Renewable and Sustainable Energy Conference (IRSEC), https://doi.org/10.1109/IRSEC.2018.8702853

Masrur, H., Howlader, H. O. R., Elsayed Lotfy, M., Khan, K. R., Guerrero, J. M., & Senjyu, T. (2020). Analysis of techno-economic-environmental suitability of an isolated microgrid system located

in a remote island of Bangladesh. *Sustainability*, *12*(7), 2880. https://doi.org/10.3390/su12072880

Memon, S. A., & Patel, R. N. (2021). An overview of optimization techniques used for sizing of hybrid renewable energy systems. *Renewable Energy Focus*, *39*, 1-26. https://doi.org/10.1016/j.ref.2021.07.007

Mirjat, N. H., Uqaili, M. A., Harijan, K., Walasai, G. D., Mondal, M. A. H., & Sahin, H. (2018). Long-term electricity demand forecast and supply side scenarios for Pakistan (2015–2050): A LEAP model application for policy analysis. *Energy*, *165*, 512-526. https://doi.org/10.1016/j.energy.2018.10.012

Moghaddam, M. J. H., Kalam, A., Nowdeh, S. A., Ahmadi, A., Babanezhad, M., & Saha, S. (2019). Optimal sizing and energy management of stand-alone hybrid photovoltaic/wind system based on hydrogen storage considering LOEE and LOLE reliability indices using flower pollination algorithm. *Renewable energy*, *135*, 1412-1434. https://doi.org/10.1016/j.renene.2018.09.078

Moran, C., Moylan, E., Reardon, J., Gunawan, T. A., Deane, P., Yousefian, S., & Monaghan, R. F. (2023). A flexible techno-economic analysis tool for regional hydrogen hubs–a case study for Ireland. *International journal of hydrogen Energy*, *48*(74), 28649-28667. https://doi.org/10.1016/j.ijhydene.2023.04.100

Mulenga, E., Kabanshi, A., Mupeta, H., Ndiaye, M., Nyirenda, E., & Mulenga, K. (2023). Techno-economic analysis of off-grid PV-Diesel power generation system for rural electrification: A case study of Chilubi district in Zambia. *Renewable energy*, *203*, 601-611. https://doi.org/10.1016/j.renene.2022.12.112

Mulumba, A. N., & Farzaneh, H. (2023). Techno-economic analysis and dynamic power simulation of a hybrid solar-wind-battery-flywheel system for off-grid power supply in remote areas in Kenya. *Energy Conversion and Management: X*, *18*, 100381. https://doi.org/10.1016/j.ecmx.2023.100381

N'guessan, S. A., Agbli, K. S., Fofana, S., & Hissel, D. (2020). Optimal sizing of a wind, fuel cell, electrolyzer, battery and supercapacitor system for off-grid applications. *International journal of hydrogen Energy*, *45*(8), 5512-5525. https://doi.org/10.1016/j.ijhydene.2019.05.212

Nadaleti, W. C., Dos Santos, G. B., & Lourenço, V. A. (2020). The potential and economic viability of hydrogen production from the use of hydroelectric and wind farms surplus energy in Brazil: A national and pioneering analysis. *International journal of hydrogen Energy*, *45*(3), 1373-1384. https://doi.org/10.1016/j.ijhydene.2019.08.199

NEPRA. (2020). *National Electric Power Regulatory Authority, Pakistan*. https://rise.esmap.org/data/files/library/pakistan/Renewable%20Energy/Pakistan_Annual%20Report,%20National%20Electric%20Power%20Authority_%202020-21.pdf

NEPRA. (2023). *National Electric Power Regulatory Authority, Pakistan*. https://www.nepra.org.pk/publications/Annual%20Reports/Annual%20Report%202023-24.pdf

Ngila, A., & Farzaneh, H. (2023). Techno-economic analysis and dynamic power simulation of a hybrid solar-wind-battery-flywheel system for off-grid power supply in remote areas in Kenya introduction. *Energy Convers Manag X*, *18*, 100381. https://doi.org/10.1016/j.ecmx.2023.100381

Nikolaidis, P., & Poullikkas, A. (2017). A comparative overview of hydrogen production processes. *Renewable and Sustainable Energy Reviews*, *67*, 597-611. https://doi.org/10.1016/j.rser.2016.09.044

Patel, A. M., & Singal, S. K. (2019). Optimal component selection of integrated renewable energy system for power generation in stand-alone applications. *Energy*, *175*, 481-504. https://doi.org/10.1016/j.energy.2019.03.055

Phurailatpam, C., Rajpurohit, B. S., & Wang, L. (2018). Planning and optimization of autonomous DC microgrids for rural and urban applications in India. *Renewable and Sustainable Energy Reviews*, *82*, 194-204. https://doi.org/10.1016/j.rser.2017.09.022

Samy, M., Barakat, S., & Ramadan, H. (2020). Techno-economic analysis for rustic electrification in Egypt using multi-source renewable energy based on PV/wind/FC. *International journal of hydrogen Energy*, *45*(20), 11471-11483. https://doi.org/10.1016/j.ijhydene.2019.04.038

Sanajaoba, S. (2019). Optimal sizing of off-grid hybrid energy system based on minimum cost of energy and reliability criteria using firefly algorithm. *Solar Energy*, *188*, 655-666. https://doi.org/10.1016/j.solener.2019.06.049

Seedahmed, M. M., Ramli, M. A., Bouchekara, H. R., Shahriar, M. S., Milyani, A. H., & Rawa, M. (2022). A techno-economic analysis of a hybrid energy system for the electrification of a remote cluster in western Saudi Arabia. *Alexandria Engineering Journal*, *61*(7), 5183-5202. https://doi.org/10.1016/j.aej.2021.10.041

Sen, R., & Bhattacharyya, S. C. (2014). Off-grid electricity generation with renewable energy technologies in India: An application of HOMER. *Renewable energy*, *62*, 388-398. https://doi.org/10.1016/j.renene.2013.07.028

Shahzad, M. K., Zahid, A., ur Rashid, T., Rehan, M. A., Ali, M., & Ahmad, M. (2017). Techno-economic feasibility analysis of a solar-biomass off grid system for the electrification of remote rural areas in Pakistan using HOMER software. *Renewable energy*, *106*, 264-273. https://doi.org/10.1016/j.renene.2017.01.033

Shaikh, A., Shaikh, P. H., Khatri, S. A., Saeed, M., Shah, H., & Kumar, L. (2025). Performance Optimization in Lead-Free Perovskite Solar Cell: A Comparative Approach. *IEEE Access*. https://doi.org/10.1109/ACCESS.2025.3543244

Shaikh, A., Soomro, A. M., Kumar, M., & Shaikh, H. (2022). Assessment of a stand-alone hybrid PV-hydrogen based electric vehicle charging station model using HOMER. *Journal of Applied Engineering & Technology (JAET)*, *6*(1), 11-20. https://doi.org/10.55447/jaet.06.01.59

Singh, A., Sharma, A., Rajput, S., Bose, A., & Hu, X. (2022). An investigation on hybrid particle swarm optimization algorithms for parameter optimization of PV cells. *Electronics*, *11*(6), 909. https://doi.org/10.3390/electronics11060909

Singh, S., Singh, M., & Kaushik, S. C. (2016). Feasibility study of an islanded microgrid in rural area consisting of PV, wind, biomass and battery energy storage system. *Energy Conversion and management*, *128*, 178-190. https://doi.org/10.1016/j.enconman.2016.09.046

Sultan, H. M., Menesy, A. S., Kamel, S., Korashy, A., Almohaimeed, S., & Abdel-Akher, M. (2021). An improved artificial ecosystem optimization algorithm for optimal configuration of a hybrid PV/WT/FC energy system. *Alexandria Engineering Journal*, *60*(1), 1001-1025. https://doi.org/10.1016/j.aej.2020.10.027

Von Colbe, J. B., Ares, J.-R., Barale, J., Baricco, M., Buckley, C., Capurso, G., Gallandat, N., Grant, D. M., Guzik, M. N., & Jacob, I. (2019). Application of hydrides in hydrogen storage and compression: Achievements, outlook and perspectives. *International journal of hydrogen Energy*, *44*(15), 7780-7808. https://doi.org/10.1016/j.ijhydene.2019.01.104

Wang, D., & Grimmelt, M. (2023). Climate influence on the optimal stand-alone microgrid system with hybrid storage–a comparative study. *Renewable energy*, *208*, 657-664. https://doi.org/10.1016/j.renene.2023.03.045

Yang, H., Zhou, W., Lu, L., & Fang, Z. (2008). Optimal sizing method for stand-alone hybrid solar–wind system with LPSP technology by using genetic algorithm. *Solar Energy*, *82*(4), 354-367. https://doi.org/10.1016/j.solener.2007.08.005

Zakeri, B., & Syri, S. (2015). Electrical energy storage systems: A comparative life cycle cost analysis. *Renewable and Sustainable Energy Reviews*, *42*, 569-596. https://doi.org/10.1016/j.rser.2014.10.011

Zarate-Perez, E., Rosales-Asensio, E., Gonzalez-Martinez, A., De Simon-Martin, M., & Colmenar-Santos, A. (2022). Battery energy storage performance in microgrids: A scientific mapping perspective. *Energy Reports*, *8*, 259-268. https://doi.org/10.1016/j.egyr.2022.06.116

Zhang, W., Maleki, A., Rosen, M. A., & Liu, J. (2018). Optimization with a simulated annealing algorithm of a hybrid system for renewable energy including battery and hydrogen storage. *Energy*, *163*, 191-207. https://doi.org/10.1016/j.energy.2018.08.112

Zhang, W., Maleki, A., Rosen, M. A., & Liu, J. (2019). Sizing a stand-alone solar-wind-hydrogen energy system using weather forecasting and a hybrid search optimization algorithm. *Energy conversion and management*, *180*, 609-621. https://doi.org/10.1016/j.enconman.2018.08.102

Zia, M. F., Elbouchikhi, E., Benbouzid, M., & Guerrero, J. M. (2019). Energy management system for an islanded microgrid with convex relaxation. *IEEE Transactions on Industry Applications*, *55*(6), 7175-7185. https://doi.org/10.1109/TIA.2019.2917357